The role of the γTuRC subunit GCP8 in microtubule regulation and cytoskeleton organization

Sabine Klischies

Tesi doctoral UPF/2015

Director de la tesi**: Jens Lüders**, PhD

Cell & Developmental Biology Programme

Institute for Research in Biomedicine Barcelona

Department of Experimental and Health Sciences

Acknowledgment

The completion of my dissertation and subsequent Ph.D. has been a long journey. I never planed to stay so many years in Barcelona and now I just don't want to leave it anymore. My journey started in 2008, when I joined Jens Lüders lab as his first Bachelor student. After first struggle with my experiments I soon learned to love the field of Centrosome and Microtubules. Maybe it's cause the "father" and first scientist to describe the centrosome was German or just cause you get those amazing pictures when you stain cells for alpha tubulin. But I got hooked to microtubules and was more then excited when I was able to stay with Jens for my PhD thesis.

Therefore first and foremost I want to thank my advisor Jens Lüders. It has been an honor to be his first student in the lab. He was not only my supervisor, but my mentor and maybe even a friend. His patience, flexibility, genuine caring and concern, and faith in me during the dissertation process has been motivating, encouraging, and enlightening. Thank you for the critical reading and editions of this manuscript. I am very debt-full for everything I learnt from you scientifically and beyond the bench.

I would like to thank Anna Aragay Combas, Sebastian Maurer, Travis Stracker, Manuel Mendoza and Maria Isabel Geli for accepting to read and evaluate my work.

I would like to thank the members of my TAC: Ferran Azorín, Travis Stracker and José Aramburu, for our annual meetings, their useful comments and advices contributed to the development of this work. A special thank to José Aramburu, for being my UPF tutor. Not to forget, Joan Roig, thanks for the critical and good advise during our lab meetings.

A special thank to the entire Microtubule Organization Group for the great atmosphere in the lab, the scientific discussion, the critics, comments and ideas about my work. Thank you for all the parties, pétanque games, trips etc.

During the time, that I have been in Lüders lab, the number of lab members has changed quite a bit, but one person has been constant through out. So a special thanks to Cristina for the help, advise and the early morning antibody changes, you finally survived the time next to the German blasting loud music. Thanks that you put up with me for such a long time!

Without Rosa there wouldn't have been SabRosa. Thank you Rosa, for being such a great lab mate; flat mate; friend and sister. The coffee breaks, girls' movie nights or late night science discussion have been a great part of my time during my PhD. Your positive spirit and smile rescued not just only once my day. Thank you for watching out for me.

Everyone else from Lüders lab, past or recent members: Carlos, Artur, Francisco, Susana, Paula, Roberta, Adrina, Neus, Marco, Florian and Leila, thanks for the great time together.

To Marko and Nico, since you guys left it hasn't been the same. I miss those ice fight, bad jokes and maybe even a bit the French accent.

I would like to thank the complete ADM facility, Julien, Anna, Lidia, Maria and Seb, I spent lot of time at the microscopes and you were always around when I needed help for image acquisition or processing.

Thanks to everyone from the organizing team of the 2nd IRB Symposium: Jordi, Kader, Selma, Radek, Manuel, Eva, Laura, Lara, Andrey, Irena, Milica. It has been an amazing experience and I miss everyone of you guys! Seriously!!!!

My time in the student council was another great experience and especially working with Giorgia, Michela, Pablo, Benjamin, Sylwia, Marianno and Natalia. Work hard, play hard!

A big thanks to everybody in IRB administration and especially to: Joan J. Guinovart, Sarah Sherwood, Sílvia Aguadé, Luca Tancredi Barone and Patricia Nadal, also to the former members Clara Caminal and Maria Rovira.

I would like thank: Michela, Giorgia, Pancho, Javi, Felipe, Nerea and Jonny for being such great friends!!!

I don't know how I would have survived the time of my PhD, without my little German Barcelona family. Danke Görner, Brechmann und Maxi, dass ihr immer für mich da seid, ob aus der Nähe oder Ferne. Buziz!

Nicht zuvergessen ClaBine, Dank auch an dich Claudi, für die Jahre der Freundschaft und die super Trips zusammen!

Natürlich der größte Dank geht an meine Eltern und mein Bruder. Ich glaube ohne eure Besuche, Pakete, Liebe, Hilfe und Unterstützung hätte ich es nicht soweit gebracht. DANKE!!!

Last but not least, thank you Greg, for sharing my life, for your endless support, for your understanding, for making me smile on rainy days, for trusting in me, for your love, for everything!!

Abstract

Microtubules (MTs) are part of the cytoskeleton in eukaryotic cells and are nucleated at microtubule organizing centers (MTOCs) by the γ-tubulin ring complex (γTuRC). Apart from subunits required for γTuRC assembly, γTuRC contains additional subunits that don't seem to have structural roles and thus may have regulatory functions. An example for such a subunit is GCP8 (also known as Mozart2). GCP8 is poorly characterized, but it is the only γTuRC subunit that is not required for mitotic spindle assembly indicating that it may regulate γTuRC specifically in non-mitotic cells. Interestingly, further analysis of the GCP8 depletion phenotype suggested that GCP8 might play a role in cell adhesion and/or contractility (Lüders lab, unpublished observation), but it remained unclear whether these defects were related to regulation of γTuRC.

The goal for my PhD thesis project was to further characterize GCP8 as a subunit of the γTuRC and provide insight into its potential role in the regulation of cell adhesion and/or contractility.

By generating GCP8 truncation mutants I characterized the interaction of GCP8 with the γTuRC and identified the γTuRC interaction domain. My results suggest that GCP8, by interacting with γTuRC, regulates growth at microtubule plus ends. In addition, GCP8 has a γTuRC independent function, affecting cell adhesion and migration through regulation of myosin dependent contractility. Consistent with this role, using different fixation and pre-extraction methods I was able to show localization of GCP8 at actomyosin-containing structures in different cell types. This localization occurred independently of the γTuRC. Interestingly, changes in GCP8 expression levels did not only affect actomyosin-based contractility but were also accompanied by changes in microtubule acetylation, supporting the recent

finding that cell contractility and microtubule acetylation are co-regulated. Finally I could show that GCP8 levels are highly variable in cancer cells and affect the metastatic behavior of cancer cells in vitro and in a xenograft model in vivo.

In summary, with this project I was able to show that the role of GCP8 in the γTuRC is regulation of microtubule plus end growth and that it has an additional, γTuRC independent function in regulating the crosstalk between myosin-based contractility and microtubule acetylation, two functions critical for metastatic properties of cancer cells.

Resumen

Los microtúbulos (MTs) forman parte del citoesqueleto de las células eucariotas y son nucleados por el complejo en anillo de la γ-tubulina (γTuRC) en los centros organizadores de microtúbulos (MTOCs). Además de las proteínas estructurales que conforman el complejo existen proteínas asociadas que lo regulan. Un ejemplo sería GCP8 (también conocida como Mozart2), que aunque no ha sido aún muy estudiada, es la única subunidad conocida del γTuRC que no se requiere para la formación del huso mitótico indicando que ésta podría regular al γTuRC en interfase. Además, otros estudios han demostrado que la depleción de GCP8 podría estar asociada a la regulación en la función de adhesión y/o contractibilidad celular (datos sin publicar), pero se desconoce si estos defectos están asociados a la regulación del γTuRC.

El objetivo de mi proyecto de tesis doctoral ha sido caracterizar GCP8 como subunidad del γTuRC y estudiar su posible papel en la regulación de la adhesión y/o contractibilidad celular.

Tras generar diferentes constructos de GCP8 determiné el dominio de unión a γTuRC. Mis resultados sugieren que GCP8, asociada al complejo del γTuRC, regula la polimerización de microtúbulos, mientras que de manera independiente del mismo, afecta la adhesión y la migración celular a través de la regulación de la contractibilidad dependiente de miosina. Mediante el uso de diferentes métodos de fijación y pre-extracción pude determinar la localización de GCP8 asociada a estructuras celulares que contienen actomiosina en diferentes tipos celulares. Dicha localización es independiente del γTuRC. También observé que los cambios a nivel de expresión de GCP8 no solo afectan la contractibilidad asociada a actomiosina, sino que también afecta la acetilación de los microtúbulos,

demostrando así que tanto la contractilidad celular como la acetilación de dichos microtúbulos esta co-regulada. Finalmente, demostré que los niveles de GCP8 son altamente variables en células cancerígenas y que tienen un efecto en el comportamiento metastático de dichas células *in vitro*, así como en un modelo xenográfico *in vivo*.

En resumen, con este proyecto he podido demostrar que la función de GCP8 en el complejo del γTuRC es la regulación del crecimiento del terminal positivo de los microtúbulos. Además presenta una función independiente del γTuRC, implicada en la regulación de la contractibilidad dependiente de miosina y la acetilación microtubular, dos funciones críticas para las propiedades metastáticas en las células cancerigenas.

Abbreviations

+TIPs	plusend tracking proteins
AA	Amino Acid
Amp	Ampicillin
bp	Base Pairs
BSA	Bovine Serum Albumin
CCT	TCP-1 Ring Complex
cd	conserved domain
Cter	C-terminus
DNA	Deoxyribonucleic Acid
DTT	Dithiothreitol
E.coli DH5α	*Escherichia coli* strain DH5-alpha
EB	End-binding protein
ECM	Extra cellular matrix
EDTA	Ethylenediaminetetraacetate
EGFP	Enhanced Green Fluorescent Protein
FA	Focal adhesion
FBS	Fetal Bovine Serum
fl	full length
g	Gram/Relative Centrifugal Force
GCP	Gamma-tubulin complex protein
GCP-WD	Neural precursor cell expressed developmentally down-regulated protein 1
GDP	Guanosine diphosphate
GEF-H1	Rho/Rac guanine nucleotide exchange factor (GEF) 2
GFP	Green fluorescent protein
GTP	Guanosine triphosphate
γTuRC	γ-Tubulin Ring Complex
γTuSC	γ-Tubulin Small Complex
h	Hour
HAUS	Human augmin complex
HCl	Hydrochloric Acid
HDAC6	Histone deacetylase 6
HRP	Horseradisch peroxidase
IP	Immunoprecipitation
IQGAP1	IQ motif containing GTPase activating protein 1
IRB	Institute for Reasearch in Biomedicine
Kb	Kilobase

KCl	Potassium Chloride
kDa	Kilodalton
Km	Kanamycin
l	Liter
LB	Luria -Bertani Medium
M	Mol l^{-1}
MAP	Microtubule associated proteins
MCS	Multiple Cloning Site
MnCl	Manganese Chloride
MOPS	Morpholinopropanesulfonic acid
MT	Microtuble
MTOC	Microtuble-Organizing Center
MYPT1	Protein phosphatase 1, regulatory subunit 12A
MZT1	Mitotic spindle organizing protein 1
n.s.	not significant
NaCl	Sodium Chloride
NaOH	Sodium Hydroxide
nm	Nanometer
NP-40	Nonidet-P 40
Nter	N-terminus
p	Plasmid
PBS	Phosphate Buffered Saline
PCM	Pericentriolar material
PCR	Polymerase Chain Reaction
Rac	Ras-related protein
RhoA	Ras homolog family member A
RNAi	RNA interference
RNAse	Ribonuclease
ROCK	Rho kinase
RT	Room Temperature
s	Second
SD	Standard deviation
SDS-PAGE	Sodium dodecyl sulphate polyacrylamide gel electrophoresis
SEM	Standard error to the mean
siRNA	Small interfering RNA
SIRT2	Histone deacetylase sirtuin 2
TAE	Tris Acetate Electrophoresis Buffer
TGA	Thioglycolic acid

Table of Contents

List of figures

Introduction

1. Cytoskeleton

The cytoskeleton is an intracellular protein structure that gives the cell shape and support. It is required for cell movement, cell division and transport with in the cells. It consists of protein subunits that polymerize into fibre-like structures. Although the name implies the cytoskeleton to be stable, it continuously undergoes changes, like nucleation and depolymerisation.

There are three different forms of cytoskeletal elements in eukaryotic cells: intermediate filaments, actin microfilaments and microtubules.

Intermediate filaments are scaffold proteins and their main function is to mechanically support the cell membrane. Intermediate filaments range in diameter size between actin and microtubules and hence the name intermediate filament. Intermediate filaments are composed of smaller rods, while eight of those rods align and twist together to form the rope-like structure of the intermediate filament. Most types of intermediate filaments are cytoplasmic, only lamin is nuclear and also often used as marker for nuclear integrity. Intermediate filaments are the only subgroup of the cytoskeleton that is not involved in cell migration.

The actin cytoskeleton with subcortical localization is giving the cell rigid stiffness and together with myosin it is the most important player for cell migration. Actin, one of the most common cellular proteins, can exist as actin monomers (G-actin), which when polymerized are called F-actin. Actin fibres can either be nucleated by formins, which form a ring shape around the actin and add free actin monomers to the growing end. Another form of actin nucleation is by the Arp2/3 complex, which binds to pre-existing actin fibres and induces new actin fibre formation by branching. Actin fibres are only 3-6 nm in diameter.

Microtubules (MTs) are essential for a variety of cellular functions, such as the formation of the spindle apparatus during cell division, directional transport of

proteins and vesicles, cytoplasmic organization, cell polarization and motility (Figure 1) (Lüders and Stearns, 2007).

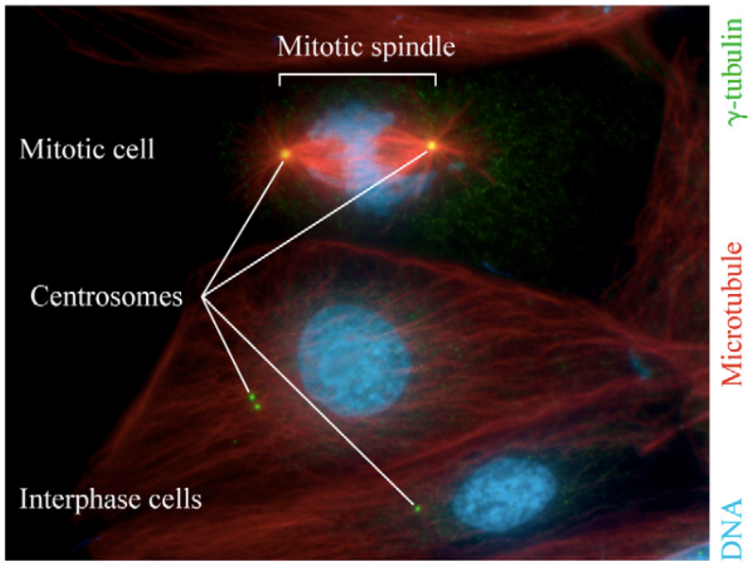

Figure 1. Typical microtubule array during interphase and mitosis.

Microtubules are shown in red, DNA in blue and γ-tubulin in green labelling the centrosome. The two different microtubule arrangements during mitosis and interphase are displayed. (From Wiese and Zheng, 2006).

1.1 Microtubules

Microtubules are hollow tubes with a diameter of 25 nm and are composed of α- and β-tubulin heterodimers that associate head-to-tail to form linear protofilaments. The microtubule is formed by 13 protofilaments through lateral association (Figure 2). The number, length, distribution and polarity of microtubules are largely determined by microtubule organizing centers (MTOCs). The proper function of the microtubule cytoskeleton depends on microtubule nucleation, elongation, stabilization and bundling, as well as severing and disassembly.

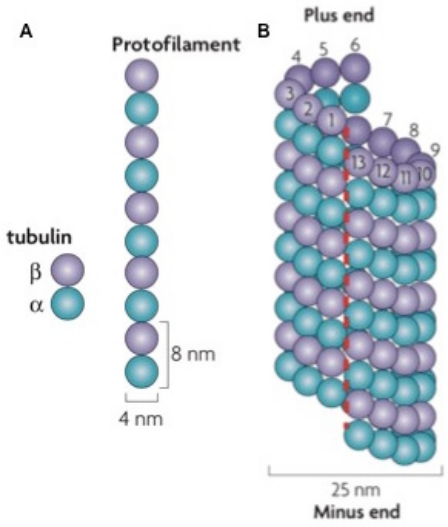

Figure 2. The microtubule structure.

(**A**)**.** Protofilaments are formed by head-to-tail interactions of α and β-tubulins. (**B**) 13 protofilaments associate laterally to form the hollow cylindrical microtubule. Adapted from (Akhmanova and Steinmetz, 2008).

1.2 Centrosome or Microtubule Organizing Center

The centrosome is the major MTOC in higher eukaryotes. Boveri has first described the centrosome already in the late 19th century. Since then, our understanding of the function and composition of the centrosome has greatly increased.

The centrosome is composed of two barrel-shaped centrioles, a mother and a daughter centriole, which are arranged perpendicular to each other (Figure 3). The centrioles are surrounded by a proteinateous matrix known as pericentriolar material (PCM) (Lüders, 2012). The PCM is the site where new MTs are formed by a process termed nucleation. During cell cycle progression the single centrosome has to be duplicated so that at cytokinesis each daughter cell receives one centrosome. Hence, the two centrioles have to disengage to allow formation of new daughter centrioles. Also the PCM undergoes changes during the cell cycle. The PCM greatly increases in size just before cells enter mitosis to nucleate additional

microtubules for robust spindle assembly (Bettencourt-Dias and Glover, 2007; Wiese and Zheng, 2006).

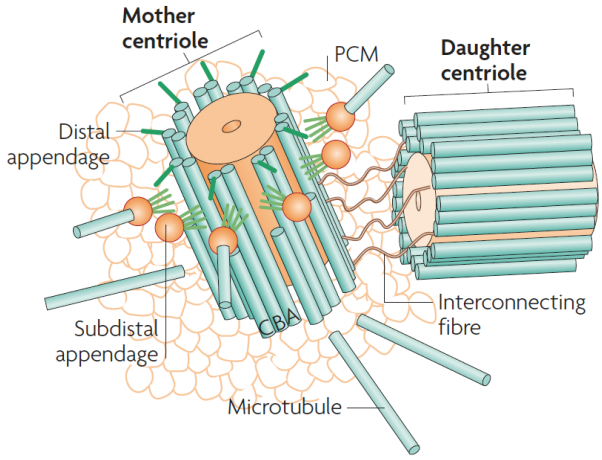

Figure 3. The Centrosome/MTOC.

Barrel shaped centrioles are composed of nine triplets of microtubules and are surrounded by the PCM, which contains γTuRC for microtubule nucleation. Adapted from (Bettencourt-Dias and Glover, 2007).

1.3 The γ-Tubulin Ring Complex and microtubule nucleation

In cells microtubule polymerization does not occur spontaneously but requires nucleation by a third tubulin, γ-tubulin. γ-Tubulin forms two different complexes: the γ-tubulin small complex (γTuSC), and a large ring-shaped complex, termed γ-tubulin ring complex (γTuRC). Each of these complexes contains several γ-tubulin molecules and additional proteins termed γ-tubulin complex proteins (GCPs).

In 2008 Kollman et al. described γTuSC in *Saccharomyces cerevisiae* as a Y-shaped heterotetrameric complex containing two molecules of γ-tubulin and one molecule each of GCP2 and GCP3, the only two GCPs present in budding yeast.

Whereas γ-tubulin is bound through the C-terminal domains of GCP2 and GCP3, they interact with each other through their N-terminal domains. In all organisms studied so far these three proteins are essential (Kollman et al., 2008)(Kollman et al., 2015) .

In mammalian cells the γTuRC is composed of ~13 γ-tubulin molecules, which are coordinated in a helical arrangement by GCP2-6 (Kollman et al., 2015). It is assumed that multiple γTuSCs associate laterally, but the positions of GCP4, GCP5, and GCP6 are not known. Recently the crystal structure of GCP4 has been solved (Guillet et al., 2011) and it has been proposed that it represents a core fold common to all GCPs (Teixido-Travesa et al., 2012). Therefore GCP4, GCP5, and GCP6 may incorporate into γTuRC by forming γTuSC-like subcomplexes.

All the GCPs (GCP2-6) and γ-tubulin are required for γTuRC assembly. Depletion of any of these components leads to disruption of the γTuRC. GCP4, 5 and 6 are not essential in Drosophila and fungi and the exact function of each of the subunits in the γTuRC is still poorly understood (Xiong and Oakley, 2009)(Verollet, 2006)(Bahtz et al., 2012).

In addition to the described γTuRC core subunits γ-tubulin and GCP2-6, NEDD1 (also known as GCP-WD) is a known γTuRC targeting factor (Lüders et al., 2006). Additional proteins were identified as novel subunits of the γTuRC, such as GCP8 (also known as Mozart2) and Mozart1. Both proteins share no sequence homology with any of the other subunits (Hutchins et al., 2010)(Teixidó-Travesa et al., 2010).

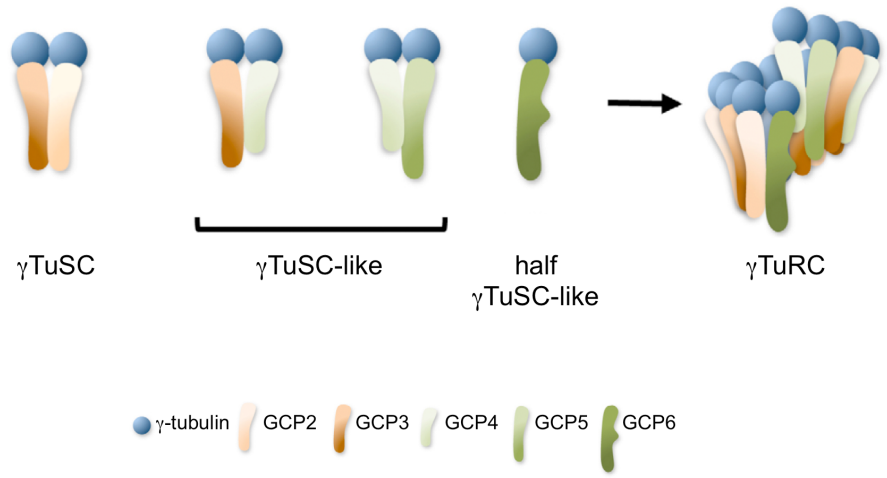

Figure 4. The γ-tubulin complexes.

γTuSC is made of GCP2 and GCP3, which each bind a γ-tubulin molecule. GCP4, 5 and 6 also associate with γ-tubulin to form similar complexes. Together with multiple γTuSCs they build the γTuRC, as can be seen in the speculative model of γTuRC assembly. (Adapted from Teixido-Travesa et al., 2012).

The main nucleator of microtubule polymerization in mammalian cells is the γ-tubulin ring complex (γTuRC).

According to the template nucleation model, the helically arranged 13 γ-tubulins on one side of the γTuRC interact with the α-tubulin subunits of α/β-tubulin dimers to initiate polymerization. In this model the γTuRC acts as a template, mimicking the end of a microtubule.

Human γTuRC is targeted by the subunit GCP-WD. GCP-WD targets γTuRC to centrosomes and also to spindle microtubules via the augmin complex (Goshima et al., 2008). Additional regulation is achieved by controlling γTuRC activity. It was suggested that γTuRC requires a specific activator. In fission yeast, the Mto1-Mto2 complex recruits but also activates the γTuRC through a conserved motif (Lynch et al., 2014). The homologue of Mto1 in higher eukaryotes is CDK5RAP2, which contains the same conserved motif. CDK5RAP2 is a centrosomal protein but is also involved in localization of the γTuRC to the Golgi (Wang et al., 2010) and was

shown to stimulate γTuRC-dependent microtubules nucleation *in vitro* and *in vivo* (Choi et al., 2010).

The recently identified γTuRC subunit Mozart1 (MZT1; GIP1 in plants) might play a role as activation factor: in plants it was shown to co-localize specifically with active γTuRC on microtubule branching sites on cortical microtubules (Nakamura et al., 2012). Also MZT1 directly interacts with GCP3 (Nakamura et al., 2012), a structural subunit that was proposed to require a conformational change to generate active γTuRC (Janski et al., 2012). Nevertheless, currently there is no direct evidence that the γTuRC is activated by MZT1 binding.

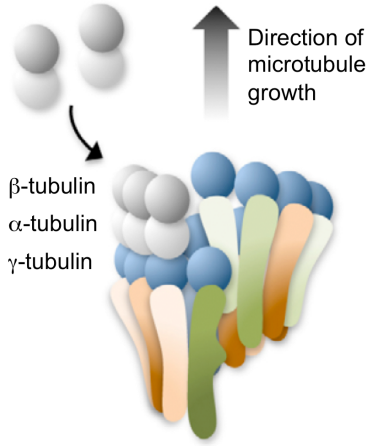

Figure 5. Microtubule nucleation, the template model.
(Taken from Teixido-Travesa et al., 2012).

2 Microtubule dynamics

Microtubules are highly dynamic structures with a rapid turn over. In cells the process of microtubule nucleation is tightly regulated whereas *in vitro* microtubules can form spontaneously. In solutions of purified tubulin with adequate supply of GTP tubulin dimers have the capacity to self-aggregate and assemble into microtubules. However, whereas microtubules in cells are composed of 13 protofilaments, the number of protofilaments in microtubules formed *in vitro* varies from 9 to 17 (Tilney et al., 1973) (Chrétien et al., 1995).

Microtubule formation *in vivo* is initiated by nucleation, followed by polymerization of α/β-tubulins dimers. The linear head-to-tail assembly of the α- and β-tubulin subunits gives microtubules an intrinsic polarity, with β-tubulin at the more dynamic 'plus' end and α-tubulin at the relatively stable 'minus' end (Akhmanova and Steinmetz, 2008). It is believed that γTuRC, by forming a cap structure, can stabilize microtubule minus ends (Wiese and Zheng, 2000).

Microtubules are mostly composed of GDP-β-tubulin, while usually the plus end of the microtubule consists of GTP-tubulin. This cap of GTP-tubulin stabilizes the microtubules, if it is hydrolyzed, microtubules rapidly depolymerize/shrink (Margolis, 1981).

Dynamic instability describes the polymerization and depolymerization of microtubules. The switch from microtubule growth to depolymerization is called catastrophe and from shrinking to growth rescue (Figure 6) (Akhmanova and Steinmetz, 2010). In between those two stages the microtubule end can pause, while the length of the microtubules is not altered.

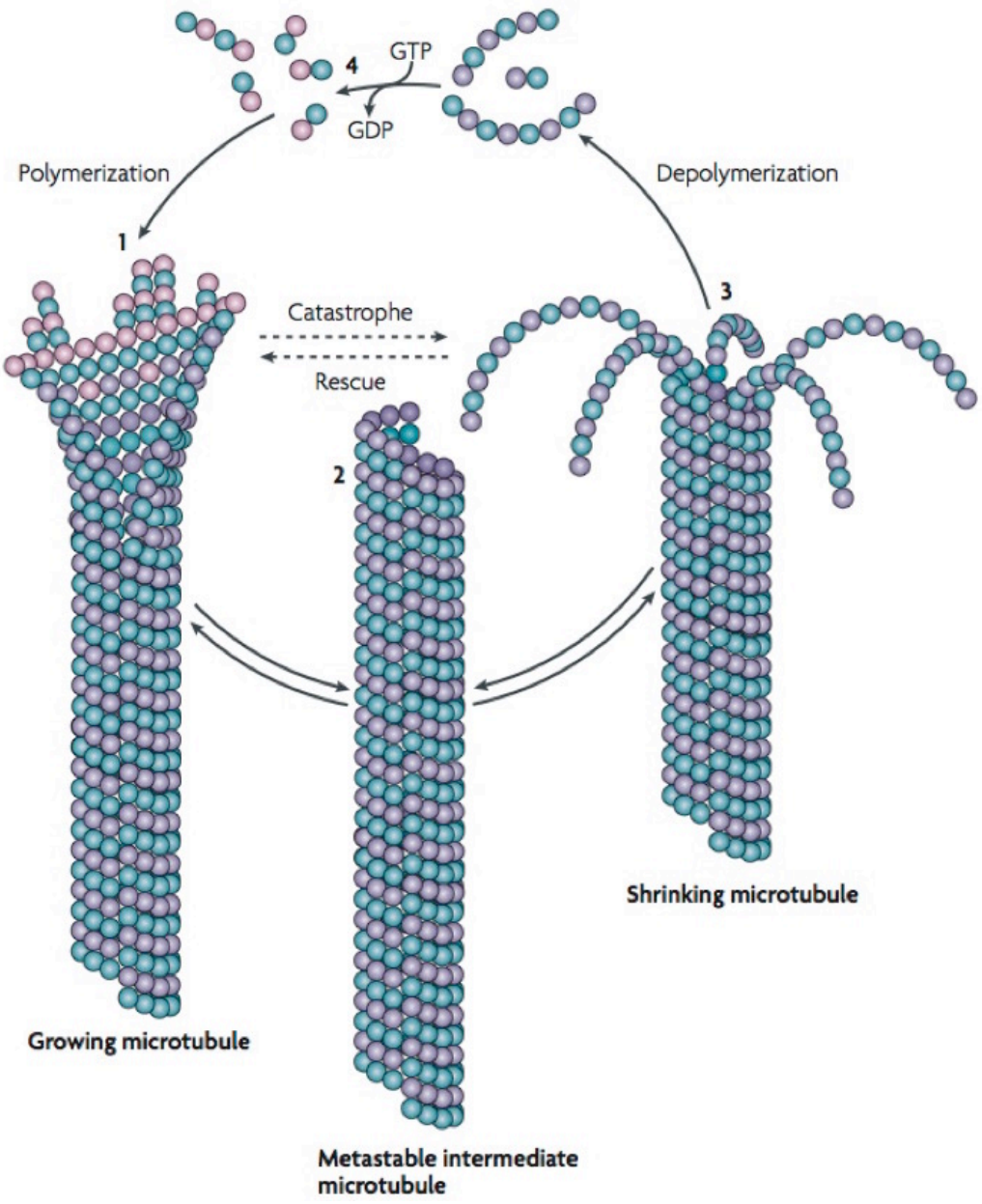

Figure 6. Microtubule Dynamic Instability.

Model showing the different stages of microtubule dynamic instability. In growing microtubules GTP-tubulin is added at microtubule plus end. The bound GTP is hydrolysed after polymerization, and therefore the microtubule lattice is mostly composed of GDP-tubulin. The change from microtubule growth to depolymerization is called catastrophe, which when reversed is called rescue. Between those two stages microtubule can pause, while the microtubule length is not altered. Adapted from (Akhmanova & Steinmetz 2008).

2.1 Factors for changing microtubule dynamics

There are different factors, which can affect the microtubule dynamics (growth and depolymerization) for example tubulin targeting drugs, microtubule associated proteins (MAPs), or post-translational modification of microtubules (PTM). For more details see the next sub chapters 2.1.1 to 2.1.4.

2.1.1 Tubulin targeting drugs

Commonly used drugs that bind to microtubules and interfere with their dynamics are Paclitaxel (Taxol), nocodazole and vincristine.

Taxol is a microtubule-binding drug and acts by stabilizing the GDP-bound tubulin in the microtubule (Arnal and Wade, 1995). So even when the GTP cap of the microtubule is hydrolyzed the microtubule doesn't depolymerize (Margolis, 1981).

Nocodazole and vincristine on the other hand have the opposite effect. They bind with high affinity the free tubulin and prevent the assembly of microtubules (Cassimeris et al., 1986). Nocodazole is also often used as microtubule depolymerizing agent. Microtubule growth is highly dynamic and if the addition of tubulin is blocked, and the existing microtubules undergo catastrophe, the complete microtubule network will eventually be depolymerized.

2.1.2 Microtubule Associated Proteins

There are two main groups of microtubule-associated proteins (MAPs), one group of proteins, which binds along the lattice of the microtubule are the structural MAPs and the other group of proteins, which are plus-end tracking proteins (+TIPs). Plus-

end binding proteins are specialized MAPs, that specifically accumulate at growing ends and can control the fate of microtubule tips.

Most of the structural MAPs are specific for nerve cells and simply stabilize microtubules by binding to the microtubule lattice, like MAP1 and Tau (Al-Bassam, 2002). MAP1 binds to microtubules by charge interaction and links the microtubule to plasma membrane. Tau also facilitates microtubule bundling and is used as an axon marker. Tau also protects microtubules from depolymerization by proteins that trigger catastrophe by hydrolyzing GTP at the plus end, such as stathmin (Baquero et al., 2012). Tau has been linked to neurological disease like Alzheimer's. In Alzheimer's disease Tau is hyper-phosphorylated and detaches from the microtubule, thus microtubules are less stable and are main cause for the symptoms in Alzheimer's disease such as dementia (Hernandez et al., 2013).

Clip-170 was the first plus-end tracking proteins (+TIPs) to be identified in 1990 (Maffini et al., 2009) (Gundersen, 2002). Since then the list of +TIPs has grown tremendously and more then 20 +TIPs families have been discovered. +TIPs in these families vary in domain composition and sizes, while they all share a common feature, the localization at the plus-end of the microtubules (Akhmanova and Steinmetz, 2010). Since all of them bind to such a small area on the microtubules, their specific function is sometimes difficult to dissect.

One of the well studied +TIP families is the EB family. EB proteins contain a highly conserved N-terminal domain, which is important for microtubule binding (Hayashi and Ikura, 2003). However EB proteins have to undergo dimerization for microtubule plus-end binding (Kim et al., 2014). GFP-tagged EB proteins are common tools in measuring microtubule dynamics. In live imaging of cells transfected with e.g. GFP-EB1 growing microtubules can be tracked by the GFP comets of EB1 on the microtubule tips (Figure 7). If then the microtubule undergoes catastrophe or pause the binding is lost and therefore also the GFP signal of GFP-EB1 at the microtubule tip.

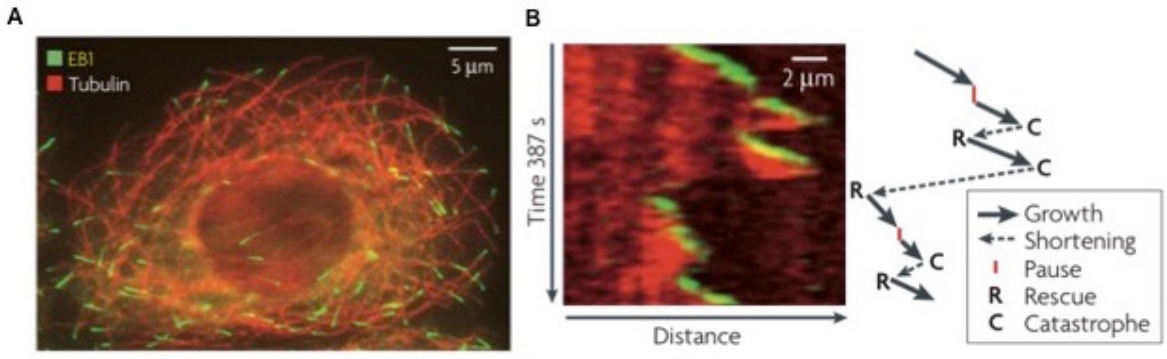

Figure 7. Localization of EB1 and microtubule plus-end tracking

(**A**) Image of an interphase cell stained for microtubules and EB1. (**B**) A kymograph which shows the different phases of microtubule dynamics an the EB1 localization. Arrows indicate microtubule growth and dashed arrows the microtubule shortening, while microtubule pausing is shown by red lines. Adapted from

2.1.3 Post-translational modification of microtubules

Microtubule dynamics and stabilization can be affected by post-translational modifications. Most of these modifications are in the C-terminal region of α-tubulin (Figure 8). This region is rich in negatively charged glutamate and forms tails that project out from the microtubule (Janke and Chloë Bulinski, 2011).

Modification of microtubules include:

- Detyrosination, a C-terminal removal of tyrosin from the α-tubulin
- Polyglutamylation, the addition of a glutamate polymer to the γ-carboxyl group of any one of five glutamates found near the end of α-tubulin
- Polyglycylation, the addition of a glycine polymer to the γ-carboxyl group of any one of five glutamates found near the end of β-tubulin and
- Acetylation, N-terminal acetylation of α-tubulin.

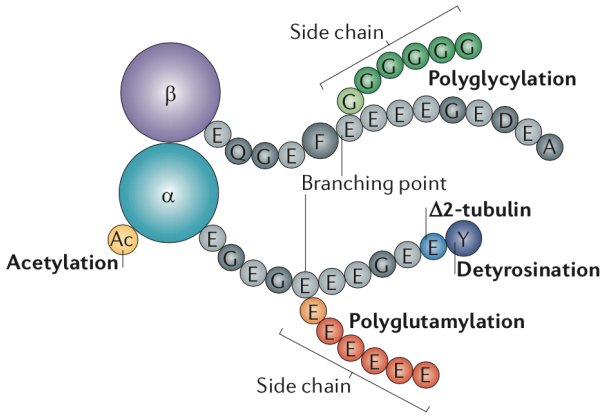

Figure 8. Post-translational modification of tubulin.

Model of the post-translational modifications of the α-tubulin–β-tubulin dimers. Adapted from Janke and Bulinski, 2011.

Since for my PhD thesis project I only studied microtubule acetylation, the next chapter explains microtubule acetylation in more detail.

2.1.4 Microtubule Acetylation

It is known that acetylation takes place on the Lys40 of α-tubulin. Recently additional acetylation sites on α-tubulin and β-tubulin have been identified in a proteome study, which are still to be confirmed *in vivo* (Choudhary et al., 2009). Numerous acetyltransferases have been shown to affect the acetylation of α-tubulin on Lys40, like: αTAT1; the ELP complex; ARD1– NAT1 and more recent MEC-17 (Janke and Chloë Bulinski, 2011).

The impact of Lys40 acetylation on any microtubule function is still unclear. It might affect microtubule function by conformational changes of the α-tubulin–β-tubulin dimer (Nakagawa et al., 2013).

Two tubulin deacetylating enzymes are known, histone deacetylase sirtuin 2 (SIRT2) and 6 (HDAC6) (Skoge et al., 2014) (Schölz et al., 2015). Both enzymes deacetylate α-tubulin and other proteins in the cytosplasm. More recently it was proposed that HDAC6 is a player in the cross-talk between cell contractility and microtubule acetylation, and is regulated by myosin phosphatase (Joo and Yamada, 2014).

3. Crosstalk between Microtubules and Actin

All individual cytoskeleton types have their distinct functions, however certain kind of cell processes require crosstalk between distinct cytoskeletal elements. For example, during cell migration, cell division and cell differentiation cooperation between microtubules and actin is needed (Akhshi et al., 2014).

3.1 Microtubule and Actin during migration

During migration cells have an elongated morphology with a front and a rear. This is achieved by a polarized organization of the microtubule cytoskeleton, while the centrosome and the microtubules re-localizes between the nucleus and the migrating front. At the leading edge protrusions are formed due to local actin assembly. This is induced by Rac, which activates the Arp2/3 complex, an actin nucleator (Ridley et al., 2003). Protrusions get in contact with the extra cellular matrix (ECM) and form new focal adhesions. Surface proteases accumulate at the protrusions adhesion sites to degrade the ECM to provide space for the cells to crawl (Keil et al., 2007). Furthermore the focal adhesion sites and the actin stress fibres in the front allow cell contractility to retract the rear. For the contractility

actomyosin activation is needed, which is regulated by Rho and ROCK (Hooper et al., 2006).

3.1.1 Microtubule turn over by Actin

In the leading edge microtubule turn over is induced by the retrograde flow of actin. The microtubules linked to actin are basically compressed and mechanically broken down (Leijnse et al., 2015).

Also actin and microtubule can be directly bound to each other via linker proteins, like the actin bound IQGAP1 that associates with the microtubule +Tip protein Clip170 (Jacquemet and Humphries, 2013), or Mip-90, a protein that interacts and binds both microtubule and actin filaments (González et al., 1998).

3.1.2 Microtubule and Focal adhesion turn over

For the cell to migrate it has to also induce a remodeling of the focal adhesion sites that connect the cell to the ECM. Existing focal adhesion sites in the rear have to disassemble to allow cell retraction and new focal adhesion sites have to be assembled in the migration front. Focal adhesions are macromolecular structures and contain integrins, which are the transmembrane connection of the cell with the ECM, and vinculin and paxillin (Yano, 2006), which serve as linker to the actin cytoskeleton. Vinculin and paxillin are typical focal adhesion markers (Ng et al., 2014).

It is known that microtubules target focal adhesions and it has been shown in a cell life imaging study in by 1999 by Kaverina et al, that the zones of FA disassembly correlates with the frequency of microtubule targeting events in the same area (Kaverina et al., 1999).

More recently, proteins were identified (CLASPs, ACF7 and APC) that directly bind microtubules to FA. All of these proteins belong to the group of +TIPs and interact trough EB1 (Kumar and Wittmann, 2012) (Lyle et al., 2009).

3.1.3 Proteins that regulate microtubules and actin

Guanine nucleotide exchange factors (GEFs) and GTPase-activating proteins (GAPs) regulate the activity of small guanine nucleotide-binding (G) proteins to control cellular functions, like cytoskeleton regulation (Bos et al., 2007).

RhoA is a small GTPase that promotes stabilization of microtubules and mediates formation of contractile actin stress fibres (Etienne-Manneville and Hall, 2002). RhoA also activates ROCK, while ROCK either directly phosphorylates myosin light chain (MLC) or inhibits the phosphatase that acts on MLC (MYPT) (Joo and Yamada, 2014), to activate myosin. The RhoA-effector Dia1 controls actin polymerization through formin and furthermore RhoA phosphorylates Tau and MAPs, which stimulates microtubule stabilization and bundling (Kitzing et al., 2007).

Rac1 belongs to the Rac subfamily of the Rho family of GTPases and regulates polymerization of both actin and microtubules to promote lamellipodial protrusion. It controls actin via Arp2/3, an actin nucleating factor (Ridley, 2001). A downstream factor of Rac1, Pak1, promotes microtubule growth by destabilizing stathmin (Wittmann, 2003).

The activity of Rho proteins is also regulated by actin and microtubules. Microtubule or actin disassembly releases bound GEF-H1, which is then available to activate RhoA (Krendel et al., 2002).

4. Cancer cell migration

Metastasis is the spreading of cancer cells from the original tumor to colonize distant sites in the host. It is a multi-step process where the cells escape from the original tumor by invading the surrounding tissue and enter the blood stream. The cells then circulate in the blood stream until they extravasate from the blood vessel at a suitable organ or tissue site, invade the surrounding tissue, and settle to produce a new tumor. During each of these steps cells have to undergo well-coordinated cytoskeletal remodeling (Gaggioli and Sahai, 2007) (Nguyen et al., 2009)(Bravo-Cordero et al., 2012).

4.1 Mesenchymal cell migration

Mesenchymal migration involves cell polarization and is based on cell protrusion and focal adhesion assembly at the front and focal adhesion disassembly and retraction at the rear. This migration mode has already been described in section 3.1 Microtubule and Actin during migration.

4.2 Amoeboid cell migration

This movement mode is named amoeboid migration since it is similar to the single cell movement of *amoeba Dictyostelium* (Friedl, 2004). Amoeboid migration has only a few loosely organized adhesion sites, therefore the cells only have weak adhesion forces and are missing the actin stress fibers (Wang et al., 2011). Motility is either based on filapodia or depends on cortical actomyosin contractile forces to remodel the cell shape by blebbing (Olson and Sahai, 2009). Usually cells using amoeboid migration are missing the proteolysis function to degrade the ECM, thus

they just squeeze forward through the ECM independent of the missing integrins or focal adhesions (Pankov et al., 2000).

4.3 Collective Cell Migration

Cells moving as a collective require intact cell-cell junctions to stay together and proteolytic activity to degrade the ECM to produce space for invasion. Furthermore they need multicellular coordination. Collective migration is based on the same principle as mesenchymal migration, but in collective migration only the cells at the leading edge form actin rich protrusions and degrade the ECM (Sahai, 2005), while the cells at the rear loss contacts with the ECM but keep the adherens junction with the other cells in the collective (Cronier et al., 2009).

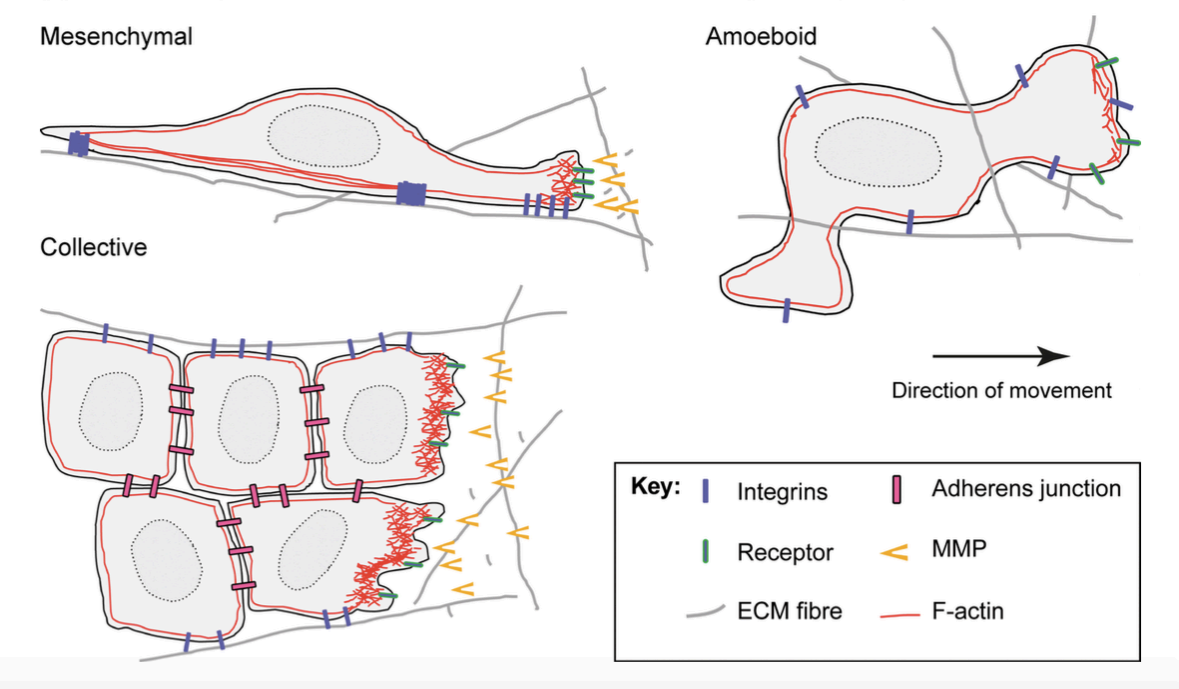

Figure 9. Mechanisms of cancer cell motility.

Schematic overview of the three different modes for cancer cell migration, mesenchymal, amoeboid and collective migration. As indicated, these migration modes vary in the distribution of integrins, adherence junctions and the actin distribution within the cells. Adapted from Sahai, 2005.

5. The γTuRC subunit GCP8, a linker between the microtubule and actin networks?

GCP8 is a rather small protein with only 18 kDa, compared to the other GCPs in the complex. It was described as a true subunit of the γTuRC, since it was co-purified with the endogenous γTuRC from Hela S3 cells and identified by mass spectrometry (Teixidó-Travesa et al., 2010).

Furthermore it co-fractionated with other subunits of the γTuRC in a sucrose gradient experiment. Moreover GCP8 was shown to co-localize with γ-tubulin at the centrosome and in the spindle during mitosis. However, depletion of GCP8 did not

disrupt the γTuRC and only caused a minor reduction of γ-tubulin at the centrosome. Hence, GCP8 is not needed for the assembly of the γTuRC or recruitment of γTuRC to the centrosome.

Additionally, depletion of GCP8 doesn't affect mitotic spindle assembly and is thus the only subunit of the γTuRC without a mitotic phenotype and might therefore play a role in microtubule organization in non-mitotic cells (Hutchins et al., 2010; Teixidó-Travesa et al., 2010).

The human genome has two GCP8 genes, which seem to be the result of a recent gene duplication. The encoded proteins GCP8A and GCP8B are more than 96% identical and both are recognized by custom-made antibodies and silenced by the siRNA that I used in this study. For all experiments involving expression of recombinant GCP8 I have used the cDNA sequence of GCP8B (Teixidó-Travesa et al., 2010).

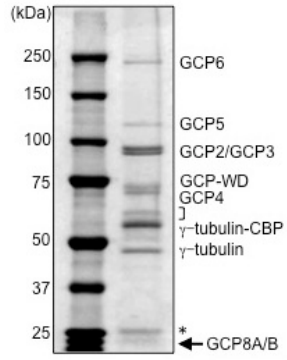

Figure 10. The γTuRC subunit GCP8.

γTuRCs purified from Hela S3 cells stably expressing TAP-tagged γ-tubulin and analysed by SDS-PAGE followed by Coomassie staining. Proteins identified by mass spectrometry are indicated. The arrow points at the subunit GCP8A/B. The asterisk marks contamination with IgG light chain, while the bracket indicates copurifying CCT chaperonin subunits. (Adapted from Teixidó-Travesa et al., 2010).

Interestingly, further analysis of the GCP8 depletion phenotype suggested that GCP8 might play a role in cell adhesion and/or contractility (Lüders lab, unpublished observation), but it remained unclear whether these defects were related to regulation of γTuRC.

6. Objectives of the thesis

Based on previous published and unpublished observation by the Lüders laboratory, the objectives of my thesis were:

i) to map the region in GCP8 that mediates binding to the γTuRC by generating GCP8 mutants,

ii) to analyze whether GCP8 may regulate the interphase microtubules network, and

iii) to investigate a potential role of GCP8 in cell adhesion and/or contractility.

Materials and methods

Molecular biology

Full-length GCP8B was PCR amplified from a human liver cDNA library using the following primers: CCGCTCGAGCGATGGCGGCGCAGGGCGTAGG and CCGGAATTCCTAGGTGCTGCCCTGCGTAGGGCT. Full-length GCP8A was PCR-amplified from plasmid pCMV-SPORT6-Fam128A (clone # 3862861; Open Biosystems, Huntsville, AL) using the same primers.

For expression in human cells amplified GCP8 sequences were inserted into pEGFP-C1 (Clontech, Palo Alto, CA) using XhoI and EcoRI restriction sites. The same restion sites and plasmid were used to clone smaller constructs of GCP8. For the expression in *Escherichia coli*, the GCP8B sequence was inserted into the pGEX-4T-1 vector (GE Healthcare, Piscataway, NJ) using EcoRI and XhoI restriction sites. Also smaller constructs of GCP8 were cloned into pEGFP-C1 (Clontech, Palo Alto, CA) using XhoI and EcoRI restriction sites. GCP8 full length and deletion mutants were sub-cloned into the XhoI and AscI restriction site of the pcDNA3-PA-Ubq-SV40-RFP, which was a generous gift from Carmen Cortina. Furthermore the same GCP8 sequences were inserted between EcoRI and BglII restriction site in the pCMV-FLAG-5, which we obtained from Joan Roig. A mutagenesis was performed with the pEGFP-GCP8 plasmid using the primer (ggcggcgctatcgaccccgaTgtAttTaaAatActCgtggacctgctgaagc) that introduced nucleotide changes in the positions in capital letters so that the expressed RNA would be resitant to GCP8 siRNA used for rescue assays.

The following plasmids were generous gifts: GFP-EB1 from Bart Lesage (IRB, Barcelona, Barcelona, Spain); GFP-MLC and GFP-Actin from Miguel Vicente-Manzanares (Universidad Autónoma de Madrid, Spain); GFP-Vinculin and GFP-Paxillin from Julien Colombelli (IRB, Barcelona, Barcelona, Spain) and GFP-Filamin A from Anna Aragay Combas (ibmb, CSIC, Barcelona, Span).

Cell Culture and treatments

Cell culture

U2OS, HEK293, RPE-1, MCF7 and Hela cell lines were grown in DMEM medium (10 % (v/v) FCS, 1 % (v/v) Penicilin/Streptaminicin) at 37 °C, 5 % CO_2 in a humidified environment. Cells were transfected with plasmid or siRNA using Lipofectamine 2000/3000 or Lipofectamine RNAiMAX (Invitrogen), respectively. For siRNA cells were analyzed after 72 hours and for plasmid transfection after 24 hours.

Stable cell line

To generate a U2OS cell line stably expressing GFP-EB1 cells were transfected with GFP-EB1 expression plasmids and selected in the presence of 0.4 μg/ml geneticin. Resistant clones were isolated and tested for expression of the tagged proteins.

Microtubule Regrowth assay

For microtubule depolymerization and regrowth experiments, cells were grown on coverslips and placed on ice for 30 minutes, for microtubule depolymerization. The coverslips with cells were then placed in DMEM at 37 °C to allow MT regrowth and were fixed at various times (0, 10 and 25 seconds) with methanol for 20 minutes at -20 °C before immunostaining.

Drug treatments

For inhibition of myosin cells were incubated with 20 μM Blebbistatin. Inhibiting of Rac1 was done with 50 μM of NSC23766 and ROCK was blocked with 10 μM of Y-27632. MTs were either stabilized by 20 μM Paclitaxel or depolimerized with Nocodazole at 20 μM. For the all the drug treatments mentioned before , I incubated the cells for 1 hour before imaging. MTs were also inhibited using Vincristine at 15 μM and protein phosphatase were inhibited with 10 μM Calyculin A, for both of these drug treatments cells were only incubated for a maximum of 20 minutes before imaging.

Invasion assay

A glass bottom 96 microscopy multiwell plate was coated with 0.2 % low of fat BSA in DMEM without phenol red, for 30 minutes at 4 °C. The collagen solution was prepared as follows: for 1 ml of final solution 713 µl collagen I, 262 µl of DMEM without phenol red and 39 µl of NaOH 0.1 M were mixed carefully. The solution was degassed before use. To degas the solution, a needle was punched trough the lid of the closed eppendorf, which was connected to the vacuum bottle in the hood. The solution was degassed for a minimum of three minutes and until all the small air bubbles rows to the top. Air bubbles were then aspirated before use. Cells were trypsinized, suspended in DMEM without phenol red and counted. Cells were mixed with collagen solution, at a concentration of 10000 cells per 100 µl collagen solution. 100 µl of cells suspended in collagen solution were placed in each well of the glass bottom 96 microscopy well plate and centrifuged at 300 g for 5 minutes in a swing out rotor. Afterwards 50 µl of DMEM with 5 % FBS were added on top and the multiwell plate was placed in an incubator at 37 °C with 10% CO_2 for 8 to 16 hours, during this time the collagen solution polimerizes. Samples were fixed with 20% formaldehyde plus 5µg/ml Hoechst 33258 (Invitrogen) directly in the well, without aspirating the media. The final concentration of formaldehyde was 4%. Fixation was done at RT with minimal disruption for at least 2 hours. Sample were then processed in the SP2 Leica microscope. Image stacks were acquired at 1 µm steps. For further image processing ImageJ software was used to reconstruct in 3D the migration distance.

CYTOOchip cell spreading assay

U2OS cells were transfected with control and GCP8 siRNA, after 60 hours cells were trypsinized, counted and diluted too a concentration of 15,000 cells per ml. CYTOOchip crossbow fibronecting coated coverslips were placed in a 6 well culture dish and 4 ml cell solution (60,000 cells) was added in each well. Cells were allowed to to settle for 10 min under the hood and then moved to the cell incubator. After 30 min the media was changed to DMEM without phenol red and the coverslip surface gently flushed to remove all the unattached cells. The

coverslips were then placed in a special holder to hold them still within the aperture of each well in a 6-well-plate. The holder was custom designed by J. Colombelli and produced by Selective Laser Sintering (SLS) out of plastic at the "Fundació Privada Centre CIM" (Barcelona). For the imaging DMEM without phenol red at 37 °C was used for the cells and the spacing between the wells were filled with warm PBS to prevent condensation on the lid and evaporation of the media. The 6 well plate with the CYTOOchips was then placed in the heated chamber of the Olympus CellR/ScanR microscope. Cells were imaged every 10 minutes for 8 hours in bright field. Images were acquired with an Orca AG camera (Hamamatsu, Bridgewater, NJ) with 10x objective. ScanR Acquisition software was used for image acquisition.

Attachment Assay

Cells transfected with plasmids or siRNA were trypsinized and counted. Per well of a 6 well plate $5x10^5$ cells were seeded in 2 ml DMEM. Cells were placed back in the incubator for either 20 or 40 minutes for attachment. At different time points media and floating cells were removed and transferred in a falcon tube and the well was washed with 2 ml of PBS, which was collected in the same tube. Cells were centrifuged and resuspended in 1 ml of DMEM and counted again. The number of cells counted gives the percentage of cells not attached after the given time points.

Wound healing assay

Cells were transected with control and GCP8 siRNA, after 64 hours cells were trypsinized, counted and $9x10^5$ cells were seeded in 2 ml DMEM per 6 well. Cells were then placed back in the incubator for 2 – 3 hours, for cells to attach and spread. When cells were 100% confluent, a (yellow) tip was used to make a straight scratch, simulating a wound. The scratch was done keeping the pipette tip under an angle of around 30 degrees to keep the scratch width limited. This allows imaging of both wound edges using the 10x objective. After the scratching the medium was changed carefully to DMEM without phenol red at 37 °C. The spacing between the wells were filled with warm PBS to prevent condensation on the lid and evaporation of the media. Cells were imaged every 10 minutes for 8 hours in bright field. Images were acquired with an Orca AG camera (Hamamatsu,

Bridgewater, NJ) with 10x objective. ScanR Acquisition software was used for image acquisition.

Antibodies

The GCP8, GCP2 and GCP4 antibodies were produced as described in Teixido et al. 2010. Other antibodies used in this study were: mouse anti-γ-tubulin (GTU-88; Sigma); mouse anti-α-tubulin (DM1A; Sigma); rabbit anti-NEDD1; mouse anti-NEDD1 (7D10, Abnova); rabbit anti-GFP (Torrey Pines Biolabs); mouse anti-GFP (3E6; Invitrogen); mouse anti-GAPDH (GAPDH 0411, Santa Cruz Biotechnology); rabbit anti-GCP3 (Proteintech group); rabbit anti-GCP6 (ab95172, abcam); mouse anti acetylated-α-tubulin (T6793, Sigma); rabbit anti-phospho-MLCII (ab2480, Abcam); mouse anti-EB1 (610534, BD Transduction Laboratories), mouse anti-Paxillin (P1093, Sigma) and mouse anti-Actin (691001, MP Biomedicals).

Alexa dye-conjugated secondary antibodies used for immunofluorescence microscopy were from Invitrogen, and peroxidase-coupled secondary antibodies for western blotting were from Jackson Immunoresearch Laboratories.

Immunoprecipitation and western blotting

For immunoprecipitation of EGFP-tagged GCP8 transfected U2OS cells were washed in PBS and lysed (50 mM HEPES, pH 7.5, 150 mM NaCl, 1 mM $MgCl_2$, 1 mM EGTA, 0.5% NP-40, protease inhibitors) for 10 min on ice. After centrifugation for 15 min at 16,000g at 4°C cleared lysates were incubated with anti-GFP antibody for 2 hours at 4°C in presence of sepharose Protein G beads. The beads were pelleted and washed three times with lysis buffer. Samples were prepared for SDS-PAGE by boiling in 1x sample buffer (0.5M Bis-Tris, 0.3M HCl, 20% glycerol, 8% SDS, 2mM EDTA, 0.06% bromophenol blue, 5%β-mercaptoethanol for the 4x sample buffer). Samples were loaded on Bis-Tris acrylamide gels (4% for stacking and 8% for separation) and run at 120mV in MOPS buffer (50 mM MOPS, 50 mM Tris-base, 0.1 % SDS, 1 mM EDTA). Proteins were transferred to membranes for 90 minutes at constant 200 mA in 1x transfer buffer (2.5mM Tris-base, 192mM

glycine, 20% methanol). Membranes were blocked in 1x TBS-T (2.5mM Tris-base, 137mM NaCl, 2.7mM KCl, 0.1% tween20 for 1ox buffer) + milk (5%) and probed with antibodies diluted in TBS-T with or without milk. Membranes were washed with TBS-T between each incubation step.

Protein Pull-Down

Full-length GCP8B was expressed and affinity-purified as a soluble GST fusion protein in *E. coli* using glutathione-sepharose (GE Healthcare), according to the manufacturer's standard protocol. Hek293 cells were harvested at 100% confluency in a 150 mm cell culture dish. Cell pellet was lysed (50 mM HEPES, pH 7.5, 150 mM NaCl, 1 mM MgCl2, 1 mM EGTA, 0.5% NP-40, protease inhibitors) for 10 min on ice. After centrifugation for 15 min at 16,000g at 4°C cleared lysates were incubated with GST or GST-GCP8 bound to glutathione-sepharose beads. The beads were pelleted and washed five times with lysis buffer. Beads were incubated in 100 µl 20 mM GSH in lysis buffer and the bound protein eluted. Samples were prepared for SDS-PAGE by boiling in 1x sample buffer (0.5M Bis-Tris, 0.3M HCl, 20% glycerol, 8%SDS, 2mM EDTA, 0.06% bromophenol blue, 5%β-mercaptoethanol for the 4x sample buffer). Samples were loaded on a Bis-Tris acrylamyde gel (4% for stacking and 8% for separation) and run at 120mV in MES buffer (50 mM MES, 50 mM Tris-base, 0.1% SDS, 1 mM EDTA). SDS Page was then stained with Coomassie blue (0.1% Coomassie Brilliant Blue R250, 50% methanol and 10% glacial acetic acid) and destained for 2 hours in (40% methanol and 10% glacial acetic acid). Bands of interest were excised from the gel and processed for Mass spectrometry.

Mass Spectrometry Analysis

Samples were in-gel digested at the facility of the PCB/IRB Barcelona and resuspended in 50 uL 1% formic acid. The nano-LC-MS/MS set up was as follows. Digested peptides were diluted in 1% FA. Samples were loaded to a 180 µm × 2 cm C18 Symmetry trap column (Waters) at a flow rate of 15 µl/min using a

nanoAcquity Ultra Performance LCTM chromatographic system (Waters Corp., Milford, MA). Peptides were separated using a C18 analytical column (BEH130TM 75 µm × 10 cm, 1.7 µm, Waters Corp.) with a 80 min run, comprising three consecutive steps with linear gradients from 1 to 35% B in 60 min, from 35 to 50% B in 5 min, and from 50 % to 85 % B in 3 min, followed by isocratic elution at 85 % B in 10 min and stabilization to initial conditions (A= 0.1% FA in water, B= 0.1% FA in CH3CN). The column outlet was directly connected to an Advion TriVersa NanoMate (Advion) fitted on an LTQ-FT Ultra mass spectrometer (Thermo). The mass spectrometer was operated in a data-dependent acquisition (DDA) mode. Survey MS scans were acquired in the FT with the resolution (defined at 400 m/z) set to 100,000. Up to six of the most intense ions per scan were fragmented and detected in the linear ion trap. The ion count target value was 1,000,000 for the survey scan and 50,000 for the MS/MS scan. Target ions already selected for MS/MS were dynamically excluded for 30 s. Spray voltage in the NanoMate source was set to 1.70 kV. Capillary voltage and tube lens on the LTQ-FT were tuned to 40 V and 120 V. Minimal signal required to trigger MS to MS/MS switch was set to 1000 and activation Q was 0.250. The spectrometer was working in positive polarity mode and singly charge state precursors were rejected for fragmentation. At least one blank run before each analysis was performed in order to ensure the absence of cross contamination from previous samples.

A database search was performed with Proteome Discoverer software v1.3 (Thermo) using Sequest search engine and SwissProt database (human release 12_03). Search parameters included trypsin enzyme specificity, allowing for two missed cleavage sites, carbamidomethyl in cysteine as static modification and methionine oxidation as dynamic modifications. Peptide mass tolerance was 10 ppm and the MS/MS tolerance was 0.8 Da. Peptides with a q- value lower than 0.1 were considered as positive identifications with a high confidence level.

Immunofluorescence Microscopy

Cells grown on coverslips were fixed in methanol at -20°C for at least 5 min and processed for immunofluorescence microscopy. Fixed cells were blocked in PBS-BT (1X PBS, 0.1% Triton X-100, 3% BSA) for 30 min and incubated with primary antibodies, followed by secondary antibodies, and finally with DAPI solution to stain the DNA. Coverslips were washed with PBS-BT between each incubation step. Antibodies/DAPI solutions were diluted in PBS-BT to their working concentration. Images were acquired with an Orca AG camera (Hamamatsu, Bridgewater, NJ) on a Leica DMI6000B microscope equipped with 1.4 NA 100x oil immersion objective. AF6000 software (Leica, Wetzlar, Germany) was used for image acquisition.

Microtubule Dynamics imaging

For MT dynamics experiments cells stably expressing GFP-EB1 were plated in glass bottom dishes. Cells were observed either treated with drugs or without in an Olympus IX81 microscope equipped with an Yokogawa CSU-X1 spinning disc and a temperature-controlled CO_2 incubation chamber. Images were acquired with a 1.4 NA 100x oil immersion objective and an iXon EMCCD Andor DU-897 camera. iQ2 software was used for the acquisition. Images were taken every 0.625 seconds as stacks (5 – 35 images, step size 1 µm).

Image processing and quantifications

For image processing and quantification of fluorescence intensities ImageJ software was used. Intensities were measured in images acquired with constant exposure settings.

For centrosomes and microtubule asters, mean intensities were measured in a circular area around centrosomes (2 µM and 5 µM diameter, respectively). For background-correction the mean intensity measured in an adjacent area in the cytoplasm was subtracted.

Kymographs were obtained, using the kymograph plugin for ImageJ. For this each time series of images was stacked and by projecting maximum intensities of the Y dimension, MT growth could then be calculated by measuring the slopes using ImageJ software.

Two-tailed, unpaired t-tests were performed for statistical analysis using Prism 6 software.

Results

1. The function of the γTuRC subunit GCP8

GCP8 was identified as a subunit of the γTuRC. Surprisingly, in contrast to depletion of other γTuRC subunits, RNAi-mediated depletion of GCP8 did not generate any mitotic spindle defects. The only defect that was observed was a slight reduction in the amount of γ-tubulin specifically at interphase centrosomes. To learn more about how GCP8 might regulate γTuRC my first goal was to identify the region of GCP8 that interacts with γTuRC.

1.1 Mapping the GCP8 binding side with the γTuRC

The mammalian GCP8 contains two conserved regions when compared to GCP8 from various species. The most highly conserved region is in the N-terminal part that is predicted to be of mainly helical secondary structure. A second, less well conserved region is found in the C-terminus. However, no known domains or sequence motifs can be identified (Teixidó-Travesa et al., 2010).

1.1.1 The N-terminus of GCP8 binds to the γTuRC

To determine the γTuRC binding region in GCP8, I designed and cloned two fragments of GCP8 tagged with GFP, separating the conserved N-terminal region from the C-terminal part. An overview of the cloned GCP8 fragments and the conserved regions is displayed in figure 14.

HEK293T cells were transiently transfected with GFP-tagged GCP8 fragments for co-immunoprecipitation experiments using anti-GFP antibodies.

Immunoblots revealed that GFP-tagged full length GCP8 (named GFP-GCP8) or an N-terminal fragment of GCP8 (amino acids 1-111; named GFP-GCP8 Nter) were able to co-precipitate the γTuRC subunits γ-tubulin and GCP6, indicating binding of these constructs to γTuRC. No binding was observed with the C-terminal GCP8 fragment (amino acids 112-158; named GFP-GCP8 Cter).

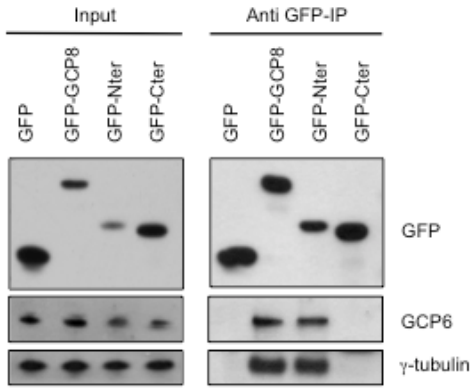

Figure 11. The N-terminus of GCP8 binds to the γTuRC

Extracts from HEK293 cells expressing GFP, GFP-GCP8, GFP-GCP8 Nter or GFP-GCP8 Cter were subjected to immunoprecipitation (IP) with anti-GFP antibody. The immunoprecipitates and the cell extracts (Input) were analyzed by western blotting (WB) with anti-γ-tubulin and anti-GCP6 antibodies.

1.1.2 Efficient γTuRC binding requires the entire N-terminal region of GCP8

To map the region in GCP8 that binds to γTuRC more precisely, I generated smaller fragments of GCP8 and used these for immunoprecipiation experiments.

However, any further reduction in the size of the GCP8 Nter fragment strongly reduced or completely eliminated the capacity to bind to the γTuRC (**Error! Reference source not found.**).

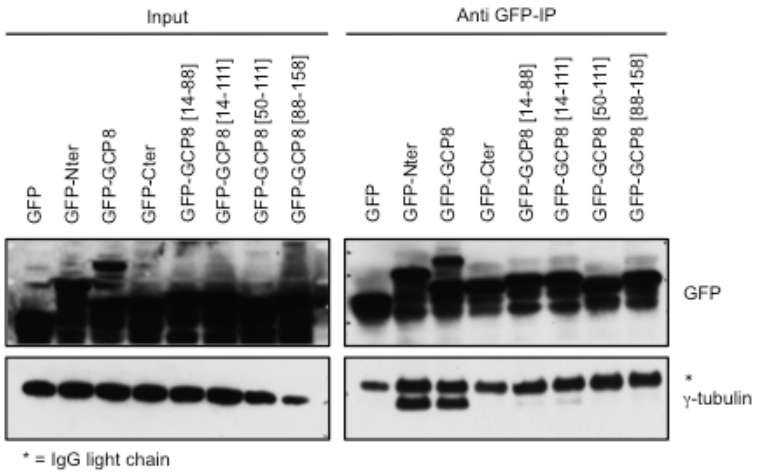

Figure 12. The entire N-terminal region of GCP8 is required for γTuRC binding.

Full length GCP8 and GCP fragments were transiently expressed in HEK293T with a GFP tag. Anti-GFP immunoprecipitates were immunoblotted with anti-GFP and anti-γ-tubulin antibodies. A summary for the binding results is shown in figure 14. The asterisk indicates cross-reactivity with the IgG heavy chain derived from the anti-GFP antibody used for immunoprecipitation.

1.1.3 The N-terminal region of GCP8 localizes to the centrosome

For testing the localization of GFP-tagged GCP8 and GCP8 fragments to the centrosome, I transiently transfected U2OS cells and stained with antibodies against GFP and γ-tubulin. Previous work from our laboratory showed that the endogenous GCP8 localizes to the centrosome in a γTuRC depended manner (Teixidó-Travesa et al. 2010). Like full length GFP-GCP8, the GFP-GCP8 Nter fragment also showed a centrosomal localization (colocalization with γ-tubulin), whereas the GFP-GCP8 Cter fragment did not localize to centrosomes (Figure).

Therefore the N-terminal region of GCP8 is important for the γTuRC binding and the centrosomal localization of GCP8.

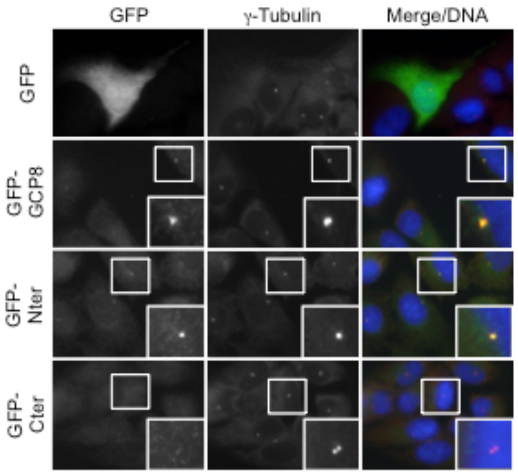

Figure 13. Full length GCP8 and the N-terminal region of GCP8 localize to the centrosome.

U2OS cells were transiently transfected with GFP, GFP-GCP8, GFP-GCP8 Nter or GFP-GCP8 Cter, fixed, and stained with antibodies against GFP and γ-tubulin. Cells with low expression levels are shown to allow visualization of centrosome localization.

A summary of the experiments probing interaction of GCP8 fragments with γTuRC and their localization to centrosomes is presented in figure 14.

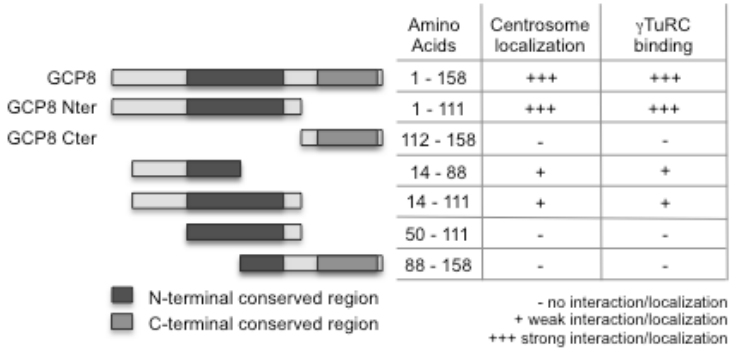

Amino Acids	Centrosome localization	γTuRC binding
1 - 158	+++	+++
1 - 111	+++	+++
112 - 158	-	-
14 - 88	+	+
14 - 111	+	+
50 - 111	-	-
88 - 158	-	-

- no interaction/localization
+ weak interaction/localization
+++ strong interaction/localization

Figure 14. Schematic overview summarizing the centrosome localization and γTuRC interaction data obtained for the different GCP8 fragments.

1.2 Roles of GCP8 in microtubule regulation

Since depletion of GCP8 did not generate any mitotic phenotype (Hutchins et al., 2010; Teixidó-Travesa et al., 2010), I focused on a potential role of GCP8 in regulating γTuRC in interphase cells.

1.2.1 Depletion of GCP8 stimulates the growth rate of microtubules

To test the hypothesis that GCP8 may have a role in regulating microtubule dynamics, I created a stable cell line expressing GFP-EB1, a microtubule +TIP that specifically labels growing plus ends of microtubules. I depleted GCP8 by transfection of siRNA and imaged microtubule plus end dynamics in live cells. I derived the parameters of microtubule dynamics from the time-lapse microscopic data of interphase cells using the *plusTipTracker* program (Applegate et al. 2011).

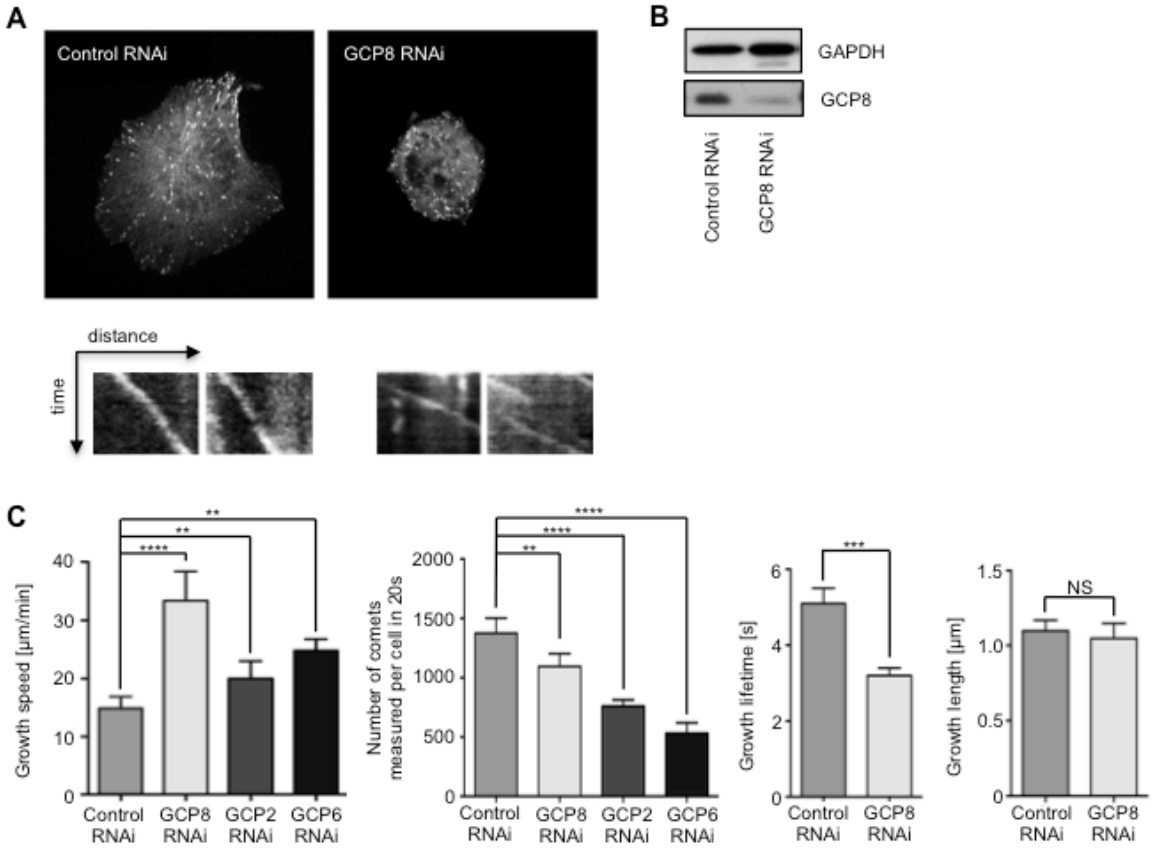

Figure 15. Depletion of GCP8 stimulates the growth rate of microtubules.

(**A**) A stable cell line expressing GFP-EB1 was transfected with control siRNA or GCP8 siRNA. The representative kymographs below the images show growth of microtubule plus ends labelled with GFP-EB1 over time. (**B**) Western blot confirming the depletion of GCP8 in cells transfected with GCP8 siRNA or the control RNAi. The protein levels of GCP8 and GAPDH, as loading control, were detected. (**C**) Mean rates of microtubule growth speed, mean number of comets measured per cell, mean growth lifetime and mean growth length measured and quantified with the *plusTipTracker* (error bars, s.e.m.; n > 150 cells from n > 10 experiments, NS, not significant; ** P < 0.01; *** P < 0.001; **** P < 0.0001).

Western blotting of U2OS cell lysates confirmed the efficient depletion of GCP8 protein levels (Figure 15, B). Total comet number in GCP8 depleted cells was slightly reduced suggesting a mild reduction in nucleation activity. Whereas the lifetime of microtubules in GCP8 depletion was reduced, while the growth length was not significantly changed. Other microtubule parameters like microtubule pause were not significantly changed (data not shown). Strikingly, I found that

depletion of GCP8 caused a profound increase in the growth speed of microtubules (Figure 15, A and C), with a shorter microtubule lifetime, while the microtubule length was not altered. As a control I also quantified microtubule dynamics in cells with disrupted γTuRC after depletion of GCP2 or GCP6. As expected, in these cells microtubule nucleation was strongly inhibited, which can be seen in the number of comets measured. The total number of comets measured in GCP2 and GCP6 were significantly reduced in comparison to the control and GCP8 depletion. However, microtubule growth rate was only slightly increased indicating that the strong stimulation of microtubule growth after depletion of GCP8 was not simply caused by a reduction in cellular nucleation activity.

I also noticed that GCP8 depleted cells had a more rounded morphology than control cells as can be seen in the still images of the Figure 15, A. Further investigations of the morphology changes are described in chapter 1.3.

1.2.2 GCP8 regulates microtubule growth rate through γTuRC.

Since GCP8 is a subunit of the γTuRC, I wanted to test whether the increase in the microtubule polymerization rate in the GCP8 depleted cells was γTuRC dependent.

I therefore chose to do a double depletion of GCP8 and either GCP2 or GCP6, to disrupt γTuRC (Figure 16).

The cells co-transfected with control RNAi and GCP8 siRNA showed an increased microtubule growth rate similar to cells transfected with GCP8 siRNA alone. Co-transfection of GCP2 or GCP6 siRNA together with GCP8 siRNA prevented this strong increase in the microtubule growth rate. Compared to controls the double depletions only slightly increased the microtubule polymerization rate.

Together these results indicate that the γTuRC is required for the increased microtubule growth rate in GCP8 depleted cells.

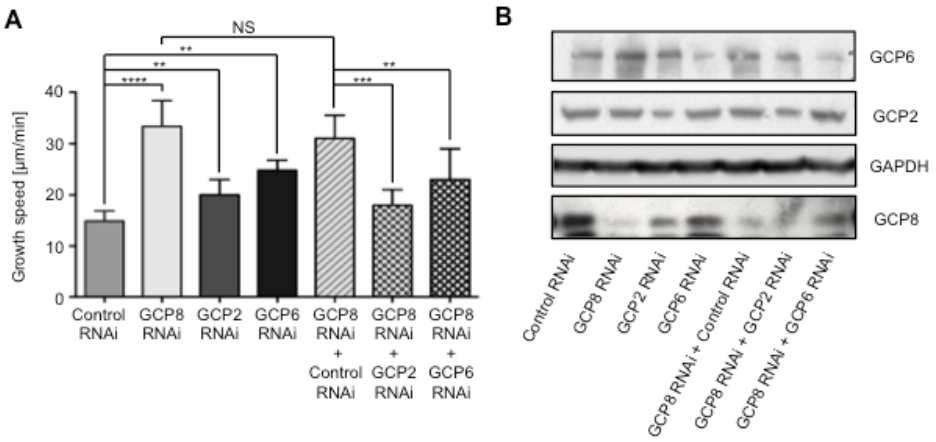

Figure 16. GCP8 regulates microtubule growth rate through γTuRC.

(**A**) Mean speed of GFP-EB1 comets in U2OS cells, imaged after 72 h of RNAi (error bars, s.e.m.; n = 20 cells for each condition; NS, not significant; ** P < 0.01; *** P < 0.001; **** P < 0.0001). (**B**) Western blot confirming the depletion of indicated proteins by siRNA or the control RNAi. The protein levels of GCP8; GCP6; GCP2 and GAPDH, as loading control, were detected.

1.2.3 GCP8 depletion increases microtubule acetylation

A change in microtubule polymerization rate might also be related to changes in the stability of microtubules. I therefore fixed and stained U2OS cells depleted of GCP8 for acetylated microtubules, a post-translational modification generally associated with more stable microtubules.

The staining for acetylated tubulin in GCP8 depleted cells revealed an increase of acetylated microtubules, which was confirmed by the fluorescent intensity measurement (Figure 17).

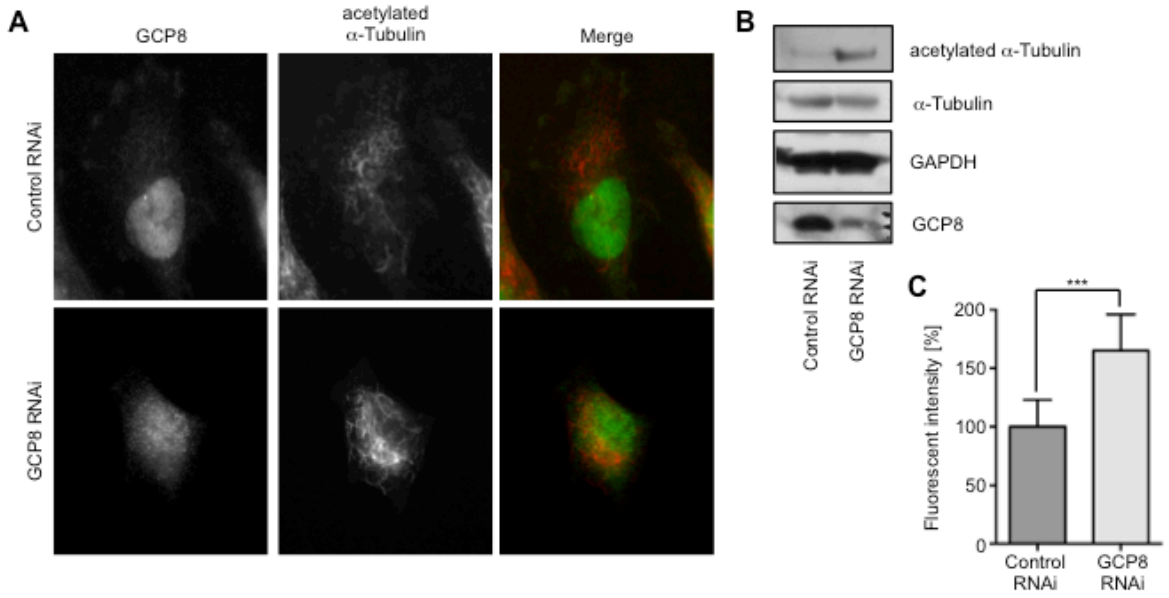

Figure 17. GCP8 depletion increases microtubule acetylation.

(**A**) U2OS cells transfected with GCP8 siRNA were fixed and stained after 72 hours with antibodies against GCP8 and acetylated α-Tubulin. (**B**) Cell lysates from control and GCP8 depleted cells were probed by immunoblotting with antibodies against GCP8, α-tubulin, acetylated α-tubulin and GAPDH, as loading control. (**C**) Mean fluorescence intensity of the acetylated α-tubulin signal in the cytoplasm of transfected cells. (error bars, s.e.m.; n > 30 cells for each condition, combined from two experiments, *** P < 0.001).

1.2.4 GCP8 over-expression also increases microtubule growth rate

Since I found that depletion of GCP8 increased both microtubule growth rate and microtubule acetylation I next determined whether over-expression of GCP8 had similar effects.

For tracking microtubule growth I transfected GCP8 fused to an RFP-tag into cells stably expressing EB1-GFP. The cells transfected with the RFP-GCP8 showed a significant increase in microtubule polymerization rate, similar to depleted cells.

To further investigate which region of GCP8 might be responsible for the increase in microtubule growth speed I also imaged EB1-GFP comets in cells expressing

RFP-Nter and Cter fragments, respectively. Interestingly, RFP-Nter, which binds to the γTuRC, increased microtubule growth speed similar to full length RFP-GCP8, whereas cells expressing the RFP-Cter fragment showed no increase in microtubule growth rate compared to cells expressing RFP as a control.

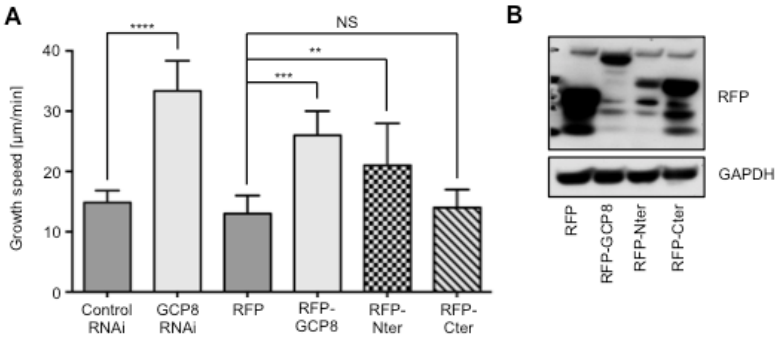

Figure 18. GCP8 over-expression also increases microtubule growth speed.

(**A**) Mean rates of microtubule growth speed of GFP-EB1 comets in U2OS cells, analyzed after 24h of transfection with the corresponding RFP construct and quantified with plusTipTracker (error bars, s.e.m.; n > 60 cells for each condition from three individual experiments ; NS, not significant; ** P < 0.01; *** P < 0.001; **** P < 0.0001) (**B**) Cell lysate from the same experiments were probed after immunoblotting for the protein levels of RFP constructs and GAPDH, as loading control.

I concluded that the increase in microtubule nucleation in GCP8 over-expression further confirms that binding of GCP8 to the γTuRC is needed, since the RFP-Nter showed a similar effect as the RFP-GCP8 overexpression.

1.2.5 GCP8 over-expression reduces microtubule acetylation.

To test if the over-expression of GCP8 also had an influence on microtubule acetylation, I fixed and stained USOS cells over-expressing either GFP or GFP-GCP8.

The over-expression of GCP8 full length tagged with GFP displayed the opposite effect as the depletion. In U2OS cells transfected with GFP-GCP8 the intensity of acetylated tubulin was decreased compared to cells transfected with the GFP

control plasmid. Furthermore the over-expression of GFP-Nter or GFP-Cter showed a similar effect with a reduction in microtubule acetylation, as the GFP-GCP8 overexpression.

Thus, whereas both depletion and overexpression of GCP8 increase microtubule growth rate, these treatments have opposite effects on microtubule acetylation and considering, that both the Nter and the Cter of GCP8 have a similar effect as GCP8, indicates that the regulation of the acetylation needs the whole GCP8.

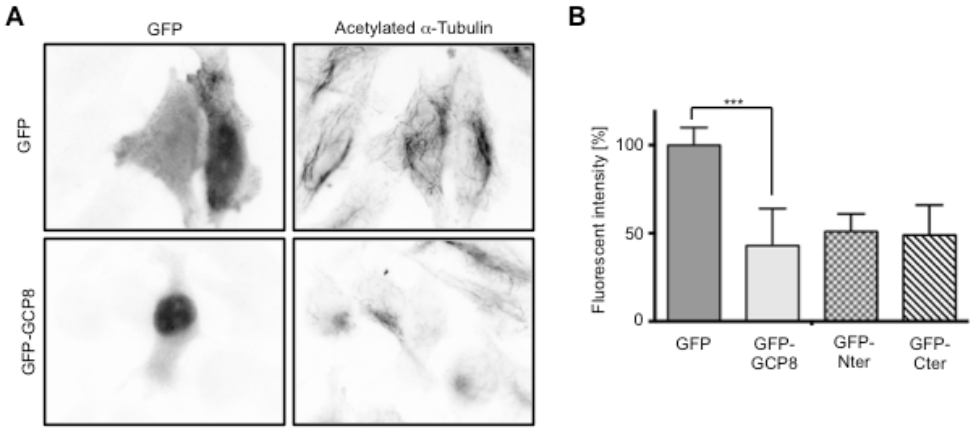

Figure 19. GCP8 over-expression decreases microtubule acetylation.

(A) U2OS cells transfected with GFP or GFP-GCP8 for 24 hours were fixed and stained with antibodies against GFP and acetylated α-tubulin. (B) Quantification of acetylated α-tubulin in the cytoplasm of transfected U2OS cells. (error bars, s.e.m.; n > 20 cells for each condition, combined from two experiments, *** P < 0.001).

1.2.6 GCP8 over-expression interferes with interphase centrosomal microtubule nucleation

Depletion of GCP8 slightly reduced nucleation at interphase centrosomes, most likely due to a slight reduction in the amount of centrosomal γ-tubulin (Teixido 2010). Since the effects of elevated levels of GCP8 on centrosomal nucleation had

not been tested, I performed microtubule regrowth assays in cells overexpressing GCP8.

Cells transfected with either GFP or GFP-GCP8 were seeded on coverslips and after a minimum of 12 hours the coverslips were placed in ice-cold water to depolymerize the microtubules. After 30 minutes of depolymerization the coverslips were transferred to warm DMEM in a 37 °C water bath, to let microtubule regrow. Coverslips were fixed in ice-cold methanol after different time points.

After 15 seconds of regrowth the GFP transfected control cells displayed robust aster formation at the centrosome, whereas cells over-expressing GFP-GCP8 had a ~50% reduction in the intensity of the microtubule asters (Figure 20).

To determine if the significant reduction in centrosomal microtubule regrowth in cells over-expressing GCP8 was due to a reduction of centrosomal proteins, I fixed and stained cells transfected either with GFP or GFP-GCP8 for different centrosomal markers.

The over-expression of GCP8 had no strong impact on the recruitment of γ-tubulin, GCP-WD and Pericentrin to centrosomes since the centrosomal levels of these proteins were similar to control cells (Figure 20).

These results suggest that increasing the levels of GCP8 does not prevent targeting of γTuRC to centrosomes but specifically inhibits centrosomal nucleation.

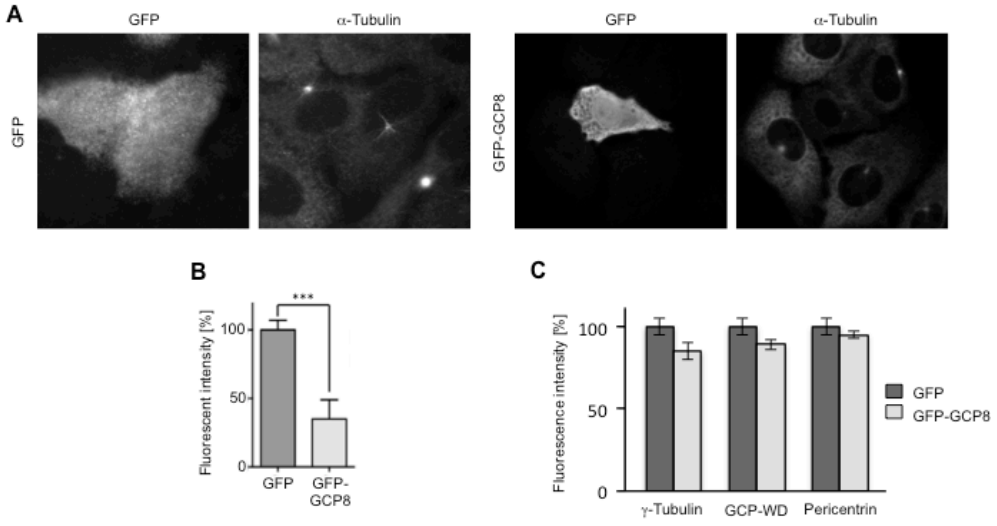

Figure 20. GCP8 over-expression interferes with interphase centrosomal microtubule nucleation.

(**A**) U2OS cells transfected with GFP or GFP-GCP8 were subjected to a microtubule regrowth assay. Microtubules were depolymerized on ice and after warming microtubules were allowed to regrow for 15 sec before fixation and staining with antibodies against GFP and α-Tubulin. (**B**) The intensities of the microtubule asters that had formed around centrosomes during regrowth were quantified and mean values were plotted as percentages of intensities in control cells (n > 20, error bars: s.e.m., *** P < 0.001). (**C**) Over-expression of GCP8 does not interfere with the recruitment of γTuRC components or centrosomal proteins to interphase centrosomes. U2OS cells transfected with either control GFP or GFP-GCP8 were stained with antibodies against various centrosome proteins. The fluorescence intensities of centrosomal signals were quantified for each of the detected proteins in interphase. Mean values are plotted as percentages of intensities in control cells, which were set to 100% (n > 20 cells, error bars: s.e.m.).

Therefore as a summary of the results for the role of GCP8 in microtubule regulation, I concluded that GCP8 specifically regulates microtubule growth in a γTuRC dependent manner. Since the results for the GCP8 depletion and overexpression have opposite effects on microtubule acetylation, these two microtubule regulations might be independent from each other.

1.3 Additional functions of GCP8

As previously mentioned, cells depleted of GCP8 had a more rounded morphology. I therefore explored whether GCP8 might have additional functions, potentially independent of the γTuRC or centrosomes.

1.3.1 GCP8 localizes to the nucleus

To address this I first re-investigated the subcellular localization of endogenous GCP8. I purified a new batch of GCP8 antibody for staining in several different cell lines, using different extraction/fixation protocols.

As can be seen in the Figure 21, I could confirm that under standard fixation conditions endogenous GCP8 co-localized with the centrosome (labeled by anti-NEDD1 antibody), centered in the typical radial microtubule array.

However, apart from the centrosomal localization the antibody also stained the nucleus.

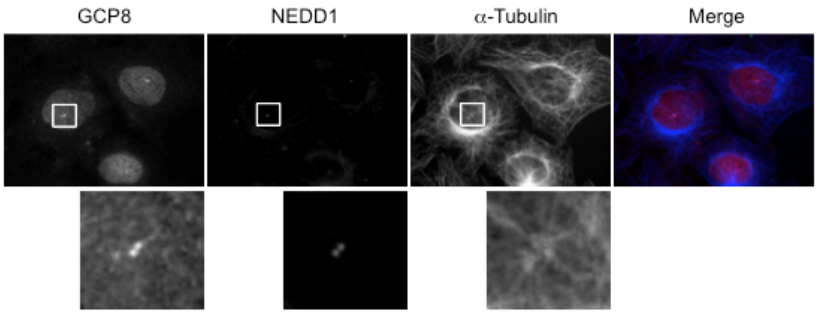

Figure 21. Typical endogenous GCP8 localization in U2OS cells.

U2OS cells were fixed in ice-cold methanol and subjected to our usual staining protocol using the indicated antibodies.

1.3.2 GCP8 co-localizes with Actin.

Next I used a pre-extraction protocol to remove soluble cytosolic GCP8 before fixation. Using this method in U2OS cells I was also able to localize the endogenous GCP8 on actin stress fibres. The end of actin stress fibres displayed a dot like localization of the endogenous GCP8. Actin stress fibres are anchored in the cells by focal adhesions, therefore the enrichment of GCP8 at the end of an actin stress fibre might indicate a co-localization of GCP8 with focal adhesions.

In addition, expression of GFP-GCP8 revealed a localization to the cell cortex, co-localizing with cortical actin. Stress-fiber localization was difficult to assess due to a more rounded morphology of cells over-expressing GCP8 compared to control cells.

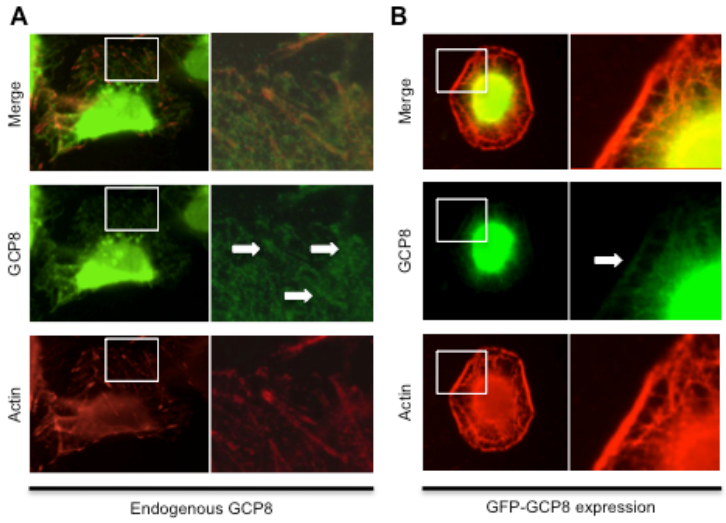

Figure 22. GCP8 co-localizes with Actin.

(**A**) U2OS cells transfected with GFP-GCP8 were pre-extracted and fixed after 24 hours of expression and stained for GFP and Actin. Arrow indicating cortical actin localization of GCP8. (**B**) U2OS were pre-extracted, fixed and stained for Actin and endogenous GCP8. Arrows indicating GCP8 co-localization with Actin stress fibers.

1.3.2 GCP8 co-localizes with Paxillin at focal adhesions

Since I saw a co-localization of GCP8 with actin stress fibres I also investigated if GCP8 also co-localizes with focal adhesions at then end of actin stress fibers. I pre-extracted U2OS cells as before and stained for GCP8 and Paxillin, a focal adhesion marker. Indeed both proteins partially co-localized (Figure 23).

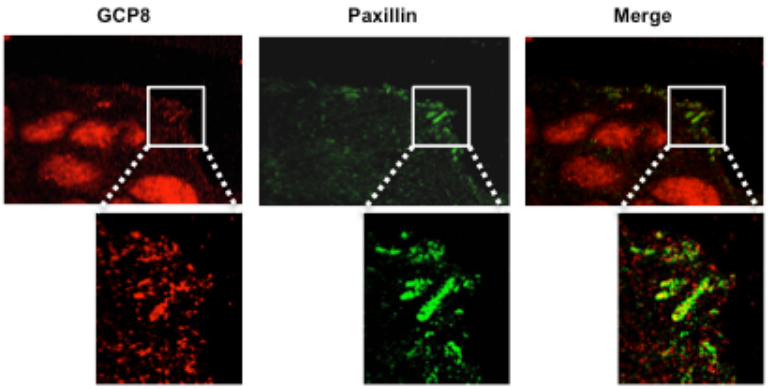

Figure 23. GCP8 co-localizes with Paxillin at focal adhesions.

U2OS cells pre-extracted, fixed and stained for endogenous GCP8 and Paxillin as focal adhesion marker. Single focal plane imaging was performed with the Leica TCS SP5 MP system.

1.3.3 The C-terminal region of GCP8 mediates localization to actomyosin-related structures like the midbody

Interestingly I also observed localization of the GFP-tagged GCP8 to the midbody region, where actomyosin-dependent constriction occurs during cytokinesis.

In U2OS cells transfected with GFP-tagged GCP8 full length or fragments, only full length GCP8 and the fragment GCP8 Cter were localizing to the midbody. GFP or the GCP8 Nter fragment, which binds to the γTuRC, did not localize as strongly to the midbody. Therefore the recruitment of GCP8 to the midbody may be mediated by the C-terminus of GCP8.

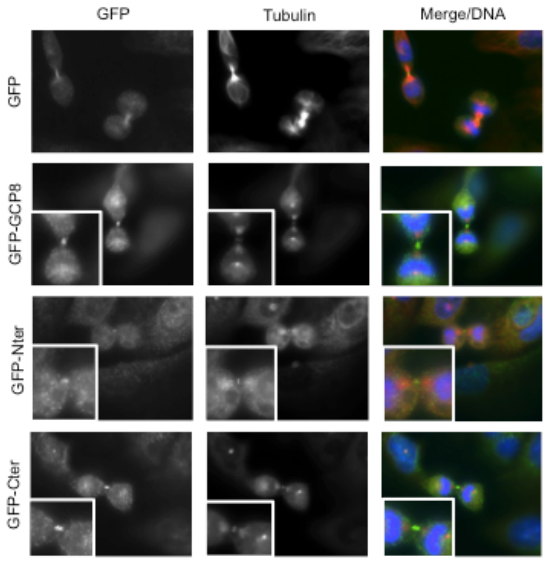

Figure 24. The C-terminal half of GCP8 mediates localization to actomyosin-related structures like the midbody

U2OS cells were transiently transfected with GFP, GFP-GCP8 or GFP-GCP8 Cter and fixed with ice-cold methanol after 24 hours of expression, followed by an immunostaining for GFP and tubulin.

1.3.4 GCP8 localizes to the cell cortex at cell-cell junctions independently of γTuRC

To study GCP8 localization in a different cell model, I obtained BM20990 cells from our collaborator Roger Gomis (IRB Barcelona). BM20990 cells are human bone metastatic cells, derived from the MCF7 breast cancer cell line. These cells express high levels of GCP8 (Figure 36) and form a monolayer with tight cell-cell contacts under standard culture conditions.

In BM20990 cells GCP8 co-localized with GCP4 to the centrosome, but, in contrast to GCP4, also displayed nuclear localization, although not as strong as in U2OS cells.

GCP8 staining also revealed additional, non-centrosomal localization. GCP8 localized at the cell cortex between cell-cell junctions.

To resolve whether the novel localization of GCP8 to the cell cortex between cell-cell junctions was γTuRC dependent, I depleted GCP2 to disrupt the γTuRC. Upon depletion of GCP2 centrosomal localization of both GCP4 and GCP8 was lost. The localization of GCP8 at the cell cortex between cell-cell junctions was only slight reduced, maybe due to co-depletion of GCP8 by GCP2 RNAi (Figure 16, B).

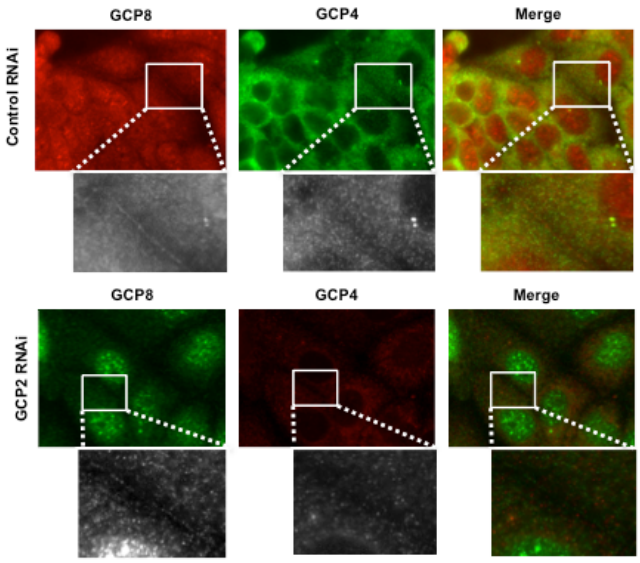

Figure 25. GCP8 localizes to cell cortex independend from the γTuRC.

BM20990 cells were transfected with control and GCP2 siRNA and fixed after 72h. Cells were stained with antibodies against the endogenous GCP8 and GCP4.

I concluded from the previous staining's, that GCP8 apart from the know localization to the centrosome also localizes to the cell nucleus, actin stress fibres and to focal adhesion sites. Furthermore also in co-localizes to actin and to the midbody region, where actomyosin-dependent constriction occurs during

cytokinesis, while the mid-body localization seems to be mediated by by the C-terminus of GCP8. Additionally in a different cell model system GCP8 staining exhibited a co-localization to the cell cortex at cell-cell junctions, independently from the γTuRC.

1.4 GCP8 and the regulation of actomyosin

1.4.1 Cells depleted for GCP8 do not adhere well to the substrate.

The localization of GCP8 to structures associated with actomyosin suggested a function of GCP8 beyond γTuRC or microtubule regulation. This hypothesis was also supported by the cell rounding that I observed upon depletion or overexpression of GCP8 and that is not a typical result of inhibition of γTuRC or microtubule function.

To determine the consequences of the observed morphological changes, I tested the ability of cells to adhere to their substrate. Control and GCP8 depleted cells were trypsinized, counted and a defined cell number was seeded into a new dish. Cells were allowed to settle and attach to the substrate for 20 or 40 minutes before unattached cells were collected.

Depletion of GCP8 strongly increased the percentage of unattached cells. After 20 min incubation only 20-30% of control cells had not yet attached to the substrate, whereas almost 80% of GCP8 depleted cells were unattached. Even after 40 minutes about half of the GCP8-depleted cells were still unattached, whereas most of the control cells adhered to the substrate at this time point (Figure 26).

To test whether the attachment defect of GCP8-depleted cells could be recued by expression of RNAi resistant tagged GCP8, control cells or cells treated with GCP8 siRNA were transfected with the GFP-tagged RNAi resistant form of GCP8 (GFP-GCP8res) and subjected to the attachment assay (Figure 26).

Indeed I observed a partial rescue of the attachment defect. However, the over-expression of the GFP-GCP8res alone also led to a slight increase in the number of unattached cells.

In summary both depletion and overexpression of GCP8 seem to interfere with the ability of cells to attach to the substrate.

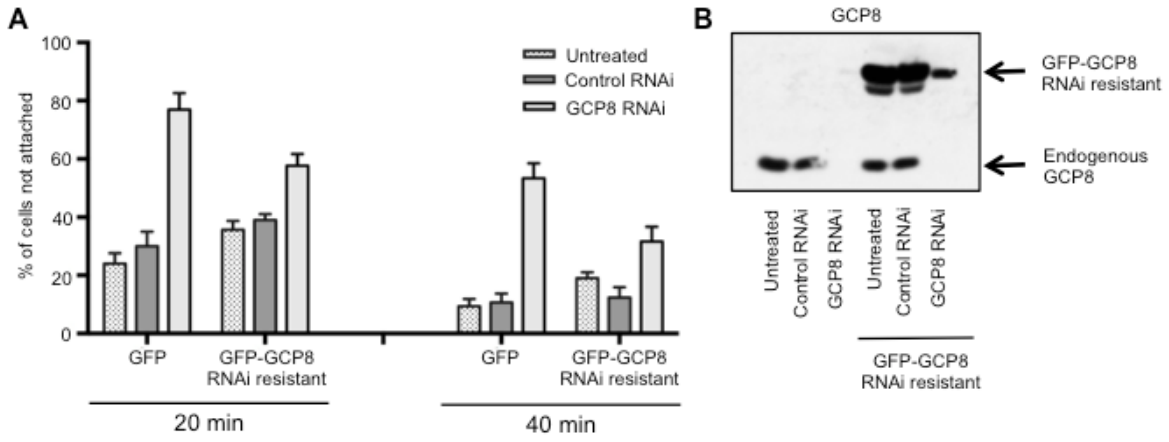

Figure 26. GCP8 depletion interferes with the attachment of cells to their substrate.

(**A**) U2OS cells were transfected with control and GCP8 siRNA for 48 hours and then transfected with GFP or GFP-GCP8res plasmid. After 24 hours cells were subjected to an attachment assay. The percentage of unattached cells after 20 or 40 min was determined and plotted. (error bars, s.e.m., n = 3 experiments) (**B**) Cell lysate from an experiment as in **A** was probed with GCP8 antibody by immunoblotting.

1.4.2 Cells over-expression GCP8 do not adhere well to the substrate.

To determine the effects of over-expression of GCP8 on cell adhesion in more detail, I repeated the assay with cells expressing GFP-GCP8 or one of the smaller fragments GCP8 Nter and GCP8 Cter.

Cells transfected with GFP-GCP8 displayed a two-fold increase of cells not attached when compared to the control only expressing GFP.

Both smaller fragments of GCP8 also inhibited attachment when expressed in U2OS cells. However, the Nter fragment caused a less severe attachment defect, while the Cter fragment impaired attachment similar to full length GCP8 (Figure 27)

To exclude the possibility, that the GFP-tag might interfere with the function of GCP8, I sub-cloned GCP8 into a vector expressing GCP8 without a tag. However,

expression of the untagged form of GCP8 induced the same attachment defect as the GFP-tagged version (**Figure** 27, B).

Therefore the lost of cell to substrate adhesion upon GCP8 over-expression seems to be regulated by the C-terminus of GCP8 and is protein tag independent.

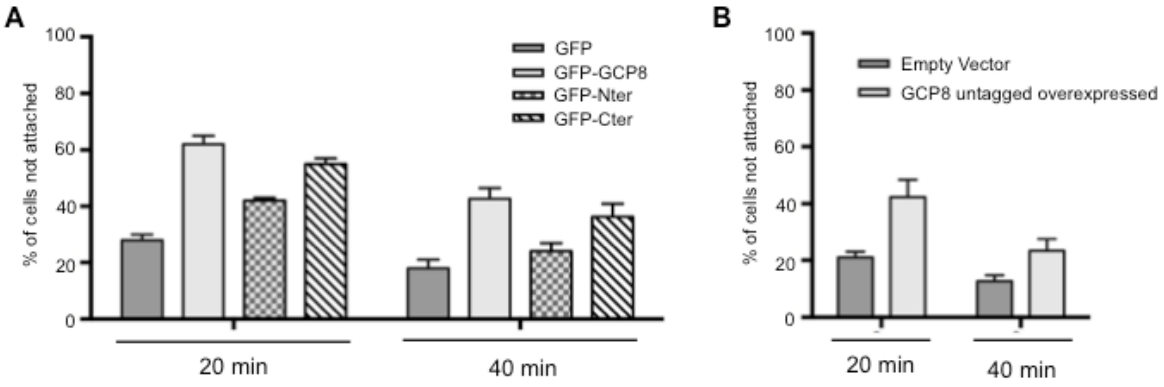

Figure 27. GCP8 over-expression interferes with the attachment of cells to their substrate. (A) U2OS cells were transfected with GFP, GFP-GCP8, GFP-GCP8 Nter and GFP-GCP8 Cter for 24 hours and then subjected to an attachment assay. (error bars, s.e.m., n = 3) (B) U2OS cells were transfected with empty vector or vector expressing untagged GCP8 for 24 hours and subjected to the attachment assay. (error bars, s.e.m.)

1.4.3 Depletion of GCP8 interferes with cell spreading after attachment.

Cells unable to adhere to the substrate surface may not be able to spread out. To test the spreading ability of cells depleted of GCP8 I seeded cells onto CYTOO chips with a crossbow fibronectin pattern. Cells were allowed to settle and the CYTOO chips were subjected to time lapse imaging for 18 hours.

Cells depleted of GCP8 presented a clear spreading defect. As can be seen in the still images of the time lapse experiment Figure , GCP8 depleted cells only covered a part of the crossbow pattern, whereas controls cells had spread over the entire pattern. At the end of the experiment the average surface covered by GCP8 depleted cells was ~50% smaller than the area covered by control cells.

Therefore GCP8 not only affects cell to surface adherence but also the cell spreading.

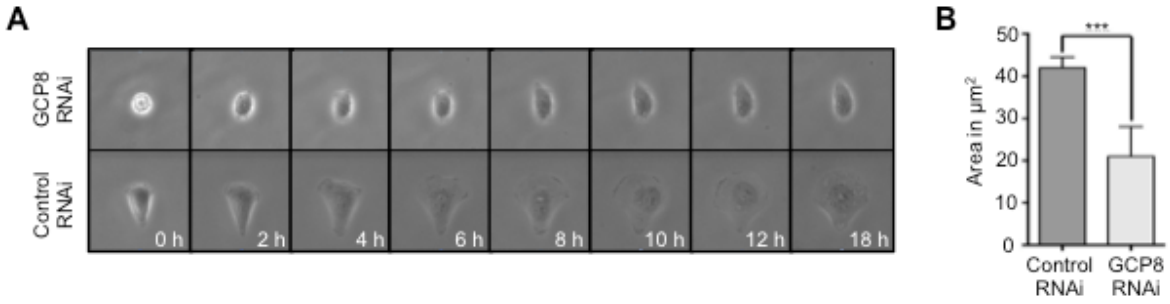

Figure 28. Depletion of GCP8 interferes with cell spreading after attachment.

(**A**) U2OS cells have been transfected with Control and GCP8 RNAi. After 64h of RNAi cells have been trypsinized and seeded on Fibronectin coated crossbow Cytoo chip for DIC real time imaging on the Olympus ScanR microscope. Still images show cell spreading during the time course of 18 hours. (**B**) Quantification of the cell area in μm^2 after 18 hours of cell attachment. (error bars, s.e.m., *** $P < 0.001$, $n > 20$ cells).

1.4.4 Reducing GCP8 levels induces membrane blebbing.

The defects in cell adhesion and spreading could be related to defects in adhesion structures, but may also be a consequence of increased cortical contractility, which could impair adhesion and spreading indirectly by inducing cell rounding. Indeed, almost 80% of the cells after GCP8 RNAi treatment exhibited extensive membrane blebbing, which was essentially absent in control cells. These membrane blebs were not caused by apoptosis, since depletion of GCP8 did not cause any increase in the percentage of apoptotic cells ((Teixidó-Travesa et al., 2010); data not shown).

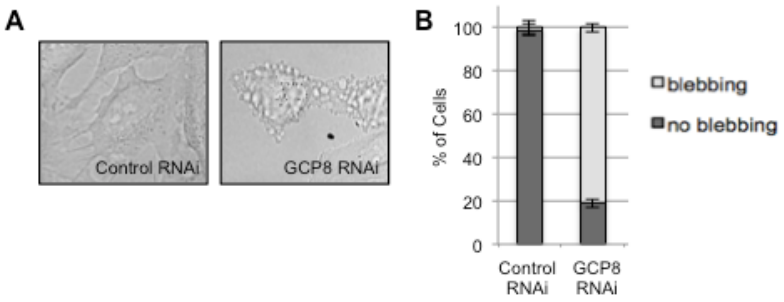

Figure 29. Reducing GCP8 levels induces membrane blebbing.

(**A**) DIC image of U2OS cells transfected with Control RNAi and GCP8 RNAi. (**B**) Percentage of cells blebbing and non blebbing for control and GCP8 depletion. (error bars, s.e.m.; n > 100 cells).

1.4.5 GCP8 overexpression also causes membrane blebbing.

Since the over-expression of the GFP-GCP8 caused an attachment defect, I consequently also quantified the number of blebbing cells in the same condition and also in cells expressing GFP-Nter or GFP-Cter.

More than 50% of the cells transfected with the GFP-GCP8 presented membrane blebbing, In the case of cells expressing GFP-Nter or GFP-Cter membrane blebbing was observed in 20% and 35% of cells, respectively. Interestingly the GFP-Cter, which does not interact with γTuRC, seems to be a stronger inducer of this phenotype.

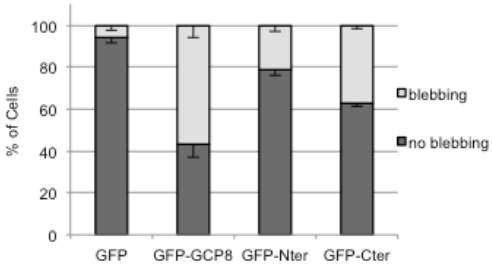

Figure 30. GCP8 overexpression also causes membrane blebbing.

Percentage of cells blebbing for transfected with GFP, GFP-GCP8, GFP-Nter, GFP-Cter. (error bars, s.e.m.; n > 100 cells).

Together with the previous data I concluded that not only GCP8 depletion, but also the over-expression of GCP8 caused membrane blebbing. Furthermore expression of the C-terminus of GCP8 exhibited a stronger blebbing phenotype, when compared to the N-terminus, which might indicate that regulation of contractility by GCP8 is γTuRC independent.

1.4.6 GCP8 depletion affects Myosin activation.

I hypothesized that the non-apoptotic membrane blebbing observed in GCP8 depleted cells may be due to an increase in cortical actomyosin activity. I analyzed by western blot cell lysates from U2OS cells transfected either with control or GCP8 siRNA. GCP8 depletion induced a strong increase in the levels of phosphorylated myosin light chain (MLC) compared to the control RNAi.

As a positive control for myosin activation, I treated cells with calyculin A, a compound that inhibits a wide range of phosphatases including myosin light chain phosphatase (MLCP) and is known to induce cortical contractility and membrane blebbing. Cells treated with Calyculin A also had high levels of phosphorylated MLC as can be seen in figure 31, B.

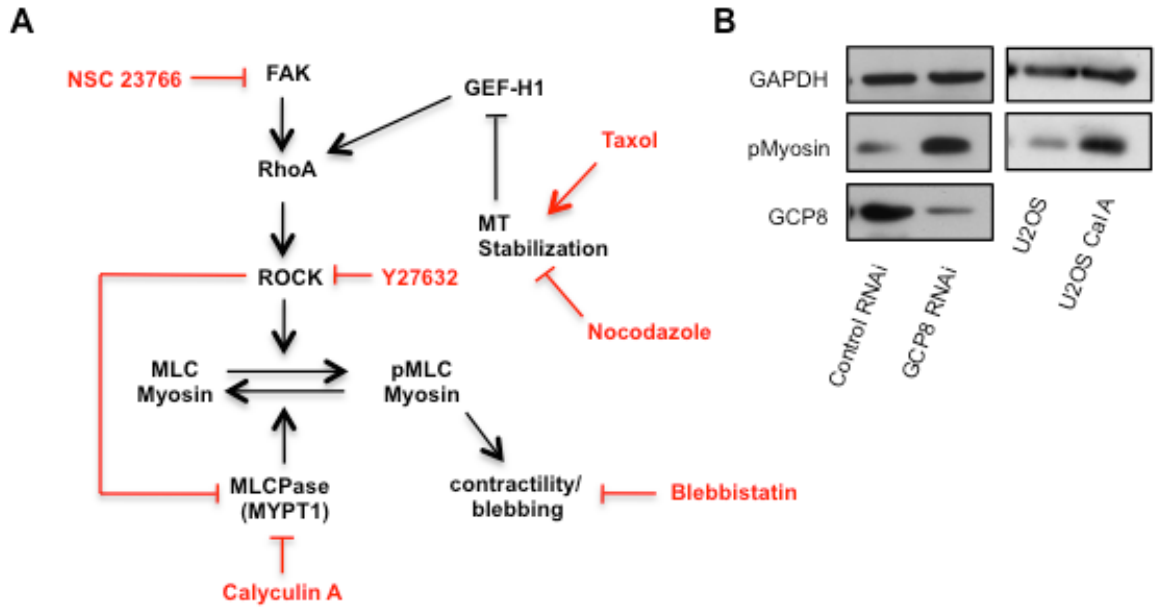

Figure 31. GCP8 depletion affects Myosin activation.

(A) The myosin activation cascade and the effects of various drugs. (B) Cell lysates from control and GCP8 depleted cells probed by immunoblotting with antibodies against GCP8, phosphorylated Myosin and GAPDH, as loading control. Control U2OS cells treated with CalyculinA were analyzed as positive control for increased cell contractility.

Together with the cell blebbing phenotype and the increase in phospho Myosin, I concluded that GCP8 depletion affects Mysoin activation.

1.4.7 Membrane blebbing induced by GCP8 depletion is myosin dependent.

To clarify at what level of the myosin activation cascade GCP8 depletion induced MLC phosphorylation, I tested the effects of various drugs on membrane blebbing in the presence or absence of GCP8 (Figure 32). The inhibitors NSC23766 and Y23632 acting on Rac/FAK and ROCK, repectively, did not abolish membrane blebbing in GCP8 depleted cells.

To further exclude that microtubules might play a role in the membrane blebbing phenotype, I used 20 nM of Taxol or 50 nM of nocodazole to reduce microtubules dynamics. The treatments with microtubule inhibitors had no detectable effect on membrane blebbing.

Finally I tested the effect of Blebbistatin. Blebbistatin is a selective cell-permeable inhibitor of non-muscle myosin II ATPases and is therefore expected to block myosin-based contractility.

In contrast to the other inhibitors blebbistatin completely blocked membrane blebbing in GCP8 depleted cells.

Together the data suggests that GCP8 may act directly on myosin rather than any of the known upstream regulators to induce membrane blebbing.

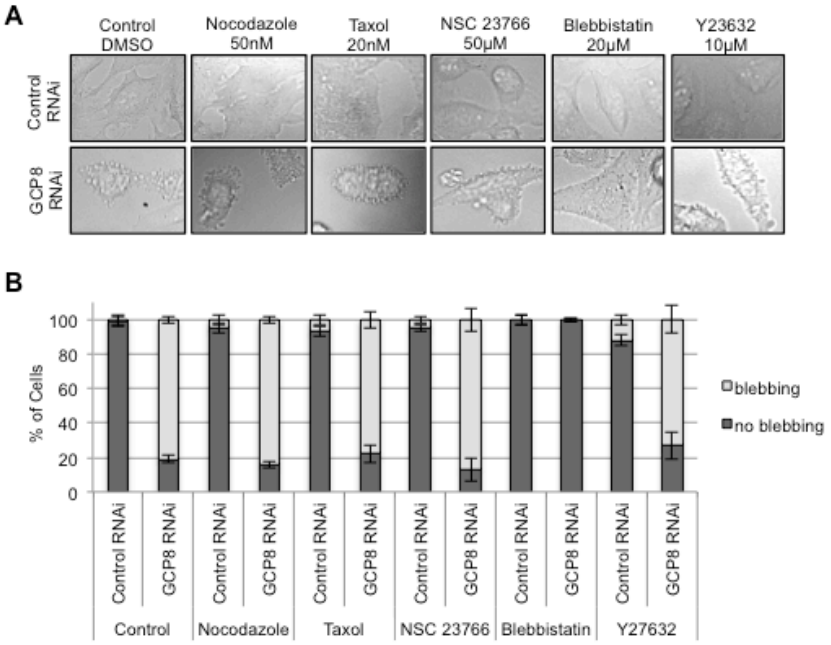

Figure 32. The effects of various inhibitors on membrane blebbing in the absence or presence of GCP8.

(**A**) U2OS control and GCP8 depleted cells treated with various drugs and imaged by DIC microscopy. (**B**) Percentage of blebbing and non-blebbing control and GCP8 depleted cells in the presence of the indicated drugs. (error bars, s.e.m.; n > 100 cells).

1.4.8 Tagged GCP8 pulls down Myosin.

Since GCP8 depletion induced MLC phosphorylation, which could only be blocked by direct inhibition of myosin using blebbistatin, I tested whether GCP8 interacted with myosin.

As first approach to test the interaction with myosin and to identify other relevant interaction partners of GCP8, I performed a protein pull-down assay. For this I expressed and purified GST or GST-tagged GCP8 from bacteria, bound the proteins to glutathione beads and incubated these with cell lysate. After several washes the bait proteins and any interaction partners were eluted from the beads with glutathione. The material was analyzed by SDS-PAGE and stained with

Coomassie blue. Bands of interest were cut out from the gel and analyzed by mass spectrometry, in the core facility of the IRB Barcelona (Figure 33, A).

Surprisingly, readily revealed by Coomassie staining, a large amount of protein seemed to be specifically associated with GST-GCP8. This was also confirmed by the mass spectrometry analysis. Among the many proteins retained on the GST-GCP8 beads were also several myosins. A compiled list with all the proteins identified in the mass spectrometry analysis can be found in the annex of the thesis.

Unexpectedly, no γTuRC subunits were identified by the mass spectrometry analysis. However, known γTuRC subunits such as γ-tubulin and GCP3 could be identified by western blotting of the material eluted from beads carrying GST-GCP8 but not GST control beads, indicating that GST-GCP8 was able to specifically pull down γTuRC from the extract (Figure 33, B).

In addition to the pull-downs I performed immunoprecipitations. I co-expressed Flag-GCP8 in combination with GFP-tagged MLC, Actin, Paxillin or Filamin and immunoprecipitated Flag-GCP8 with anti-Flag antibodies. Under these conditions Flag-tagged GCP8 co-precipitated with GFP-MLC (Figure 33, C).

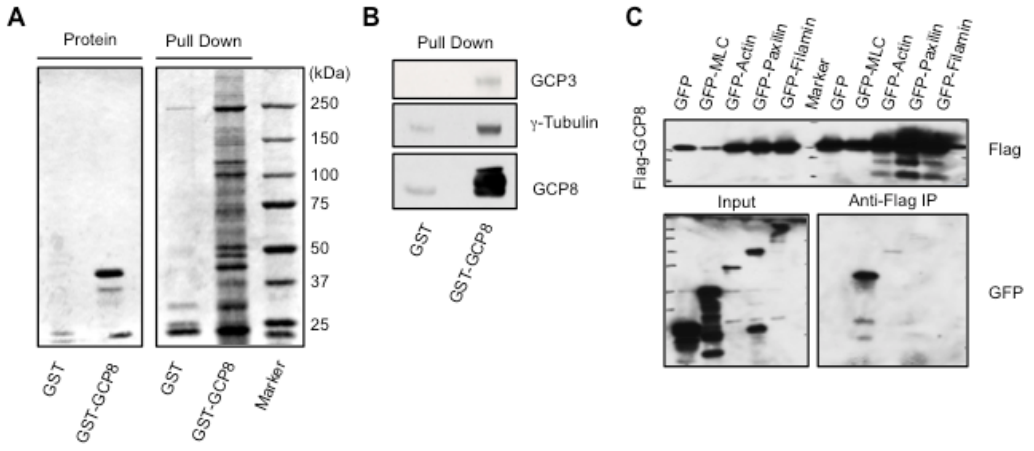

Figure 33. GST-GCP8 pulls down mutiple proteins including myosin from human cell extract.

(**A**) Coomassie staining of proteins analyzed by SDS PAGE. The left panel shows the purified proteins used for the pull-down. The right panel shows the eluted material. (**B**) The material co-eluting with GST or GST-GCP8 was probed with the indicated antibodies by western blotting. (**C**) Extracts from HEK293T cells co-expressing Flag-GCP8 in combination with GFP or GFP-tagged cytoskeleton proteins as indicated were subjected to anti-FLAG immunoprecipitation (IP). The immunoprecipitates and the cell extracts were analyzed by immunoblotting.

Together the data suggests that tagged GCP8 is able to interact with myosin complexes *in vitro.*

1.4.9 GCP8 regulates microtubule growth rate independently of cortical contractility

My data suggested that GCP8 regulates γTuRC and microtubule growth rate on the one hand and myosin-dependent cortical contractility on the other hand.

To determine if the increase in cell contractility/membrane blebbing after GCP8 depletion may be mechanistically linked to the increase in microtubule growth rate, I used blebbistain to block myosin contractility and Calyculin A to increase contractility.

Even though treatment with blebbistatin completely suppressed membrane blebbing in GCP8 depleted cells, I did not observe any change in the increased microtubule growth speed.

Cells treated with Calyculina A displayed extensive membrane blebbing, similar to the GCP8 depletion phenotype, but this did not result in an increased microtubule growth rate.

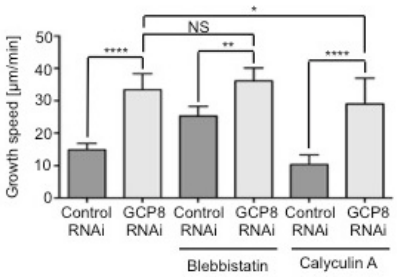

Figure 34. Regulation of microtubule growth rate by GCP8 does not depend on cortical contractility.

Mean rates of microtubule growth in U2OS cells, analyzed after 72h of transfection with the control or GCP8 siRNA and treated with either blebbistatin or Calyculina A. (error bars, s.e.m.; n > 20 cells for each condition; NS, not significant; ** P < 0.01; **** P < 0.0001).

I concluded from these results that the increase in microtubule growth rate after GCP8-depletion occurs independent of cortical contractility/membrane blebbing.

1.4.10 Manipulation of GCP8 protein levels alters cell migration and invasion.

Since myosin contractility plays a role in cell migration and invasion I tested if GCP8 depletion influences cell motility in two different assays.

First I performed a wound-healing assay using U2OS cells transfected with control or GCP8 siRNA. Cells were plated to reach confluency. A “wound” was induced by scratching the confluent cell monolayer with a pipette tip. The samples were

subjected into overnight live cell imaging. During the imaging over 12 hours the migration of cells into to wound can be observed. Control cells were able to completely close the wound after 12 hours, whereas the GCP8 depleted cells only closed the wound up to 70%.

Since the wound healing assay provides only a 2D migration environment, I decided to also employ a 3D assay, which may more closely simulate the tissue environment.

For the 3D migration/invasion assay I mixed U2OS cells transfected with either control or GCP8 siRNA with a collagen mixture and filled wells in a 96 multi-well plate with glass bottom for microscopy. After collagen polymerization FBS was added to the top of the matrix to initiate cell migration. At different time points I fixed the cells, stained with Hoechst to visualize nuclei, and analyzed cell migration by confocal sectioning.

Remarkably, in this matrix invasion assay GCP8 depletion had the opposite effect on migration as compared to the 2D wound healing assay. Cells depleted of GCP8 had migrated a greater distance into the collagen matrix than control cells (Figure 35, C and D).

I concluded that the contractile behavior of GCP8 depleted cells impaired migration in the 2D wound healing assay but promoted invasion of the 3D collagen matrix, probably by amoeboid motility.

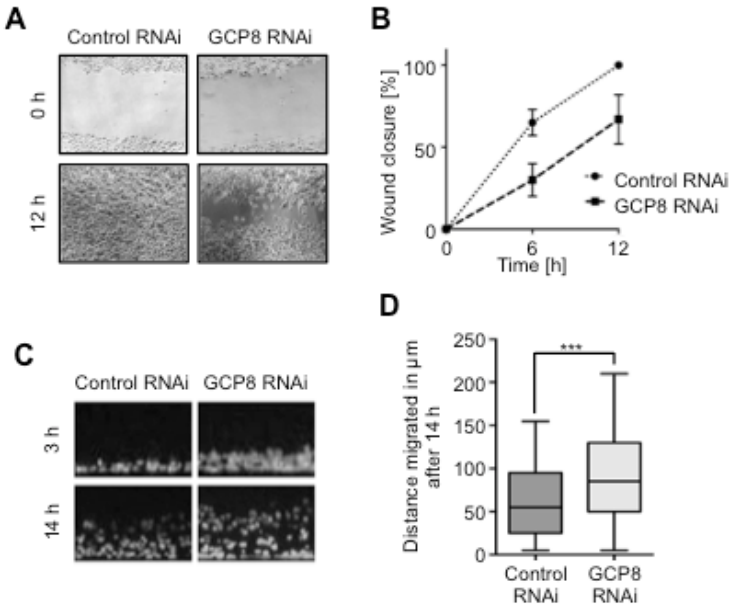

Figure 35. Manipulation of GCP8 levels alters 2D and 3D migration

(**A**) U2OS cells transfected with control or GCP8 siRNA were subjected to a 2D wound-healing assay and imaged by phase contrast microscopy. (**B**) The wound closure was quantified at 0 h, 6 h and 12 h after scratching by measuring the area that did not contain cells. Graphic represents the wound width as the mean of the % of the closure of original wound in triplicate plates.(**C**) Matrigel plugs containing cells from invasion assays were fixed and DNA was stained with Hoechst dye. Cells in confocal images are shown in cross section and side views. (**D**) Migration distance was analysed with a 3D positioning plug-in for ImageJ and the measured migration distance in µm was plotted, each box represents 50% of the cells measured. (*** $P < 0.002$; $n > 4$ experiments).

2. GCP8 and cancer

2.1 GCP8 protein levels are highly variable in cancer cells

My results suggested that GCP8 protein levels may be correlated with changes in the migratory and invasive properties of cells. Based on this observation I speculated that different cancer cells, which differ in their metastatic potential, might also display variability in GCP8 protein levels. I then analyzed different parental and derived metastatic cells lines, obtained from Roger Gomis' laboratory (IRB Barcelona), and the standard cell lines used in our laboratory, by western blotting.

GCP8 protein levels were significantly different in some sample pairs of parental versus metastatic cell lines. The BM20990 metastatic cell line, for example, had a 12 fold increase in GCP8 protein level when compared to the MCF7 parental cell line.

Moreover changes in GCP8 expression levels were not simply correlated with γTuRC abundance, since the expression of γ-tubulin was not highly variable.

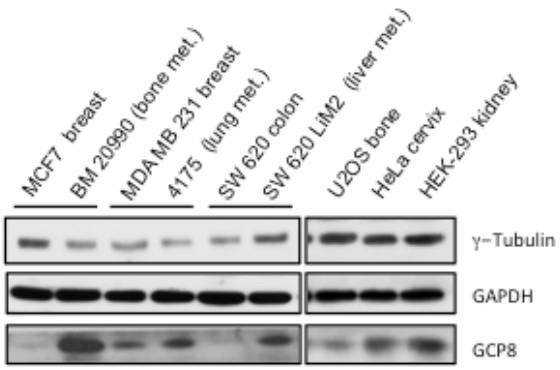

Figure 36. GCP8 protein levels are highly variable in cancer cells

Westernblot of total lysate from different cell lines (pairs of parents and derivatives that metastasize to specific organs) and from cells lines typically used in our laboratory, probed with antibodies to detect the indicated proteins.

2.2 Manipulation of GCP8 levels promotes 3D invasion of cancer cells

MCF7 cells have a relatively low protein level of GCP8 as can be seen in the previous western blot (Figure 36). To confirm that manipulation of the GCP8 protein levels also changes the 3D motility of MCF7 cells, I produced a stable MCF7 cell line overexpressing GCP8. Furthermore I also transiently depleted GCP8 in MCF7 cells to compare the effects of GCP8 over-expression and depletion in the invasion assay.

The stable cell line over-expressing GCP8 had a significantly higher ability to invade the 3D matrix compared to the control MCF7 cell line. A similar effect was observed for cells depleted of GCP8 compared to the control RNAi cells. Thus depletion or over-expression of GCP8 both altered the invasive behavior of MCF7 cells.

To test whether increased cortical contractility with blebbing might cause the enhanced invasive behavior of the MCF7 cells with altered GCP8 levels, I added

blebbistatin to the collagen matrix to inhibit myosin. The invasiveness of both cell lines MCF7 control and MCF7 GCP8 over-expressing cells was dramatically decreased.

The results suggest that the enhanced cortical contractility, induced by changes in GCP8 levels, promotes the invasive behavior of these cells.

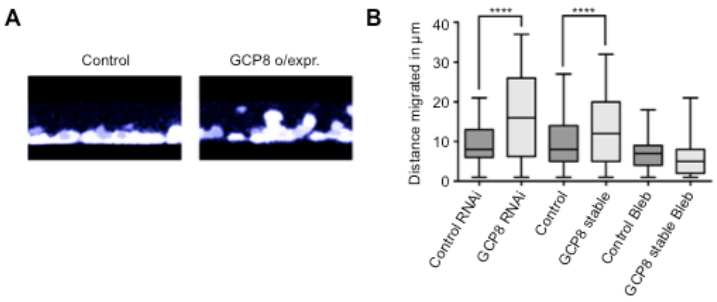

Figure 37. Manipulation of GCP8 levels promotes 3D invasion of cancer cells

(**A**) Side view of reconstructed optical sections showing control and GCP8 overexpressing cells invading the collagen matrix. (**B**) GCP8-depleted or overexpressing MCF7 cells were subjected to a 3D collagen invasion assay, stained with DAPI, and analysed by confocal optical sectioning. After 3D image reconstruction migration distances were quantified (**** $P < 0.0001$; $n = 3$ experiments).

2.3 Manipulation of GCP8 levels affects metastatic cell behavior *in vivo*

To test how manipulation of GCP8 affects cancer cells *in vivo*, I turned to a mouse bone metastasis xenograft model based on the intra-tibia injection of human MCF7 breast cancer cells stably overexpressing GCP8.

I performed the intra-tibia injection and the monitoring of the mice with the help of the Gomis' laboratory (IRB Barcelona). At 2 weeks post injection a significant

difference of cells mass could be observed. Whereas more then 50% of the mice injected with the control MCF7 cells showed bone metastasis, animals injected with GCP8-overexpressing cells were still metastasis-free. Over the time course of more then 40 days, MCF7 cells stably overexpressing GCP8 showed a strongly reduced ability to colonize bone compared to MCF7 control cells (Figure 38).

As a control, I monitored *in vitro* cell proliferation, to exclude the possibility that a reduced cell proliferation rate might have caused the decreased photon flux intensity in the tibia colonization model. I confirmed that control and GCP8-overexpressing cells proliferated at similar rates in vitro.

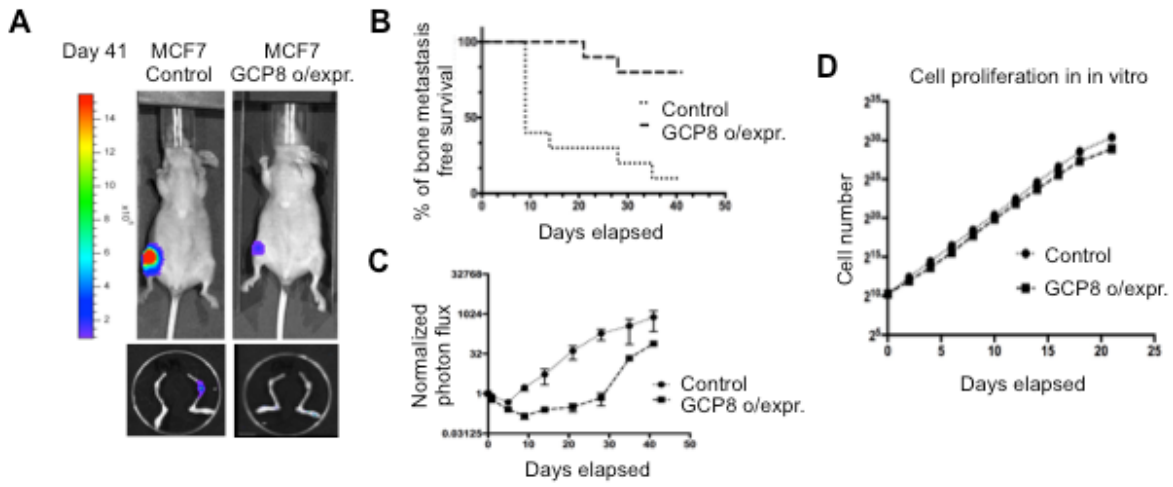

Figure 38. Manipulation of GCP8 expression levels modulates metastatic behavior of cancer cells *in vivo.*

(**A**) Mouse tibia were injected with MCF7 control and MCF7 GCP8 over-expressing cells (n=10 for each cell type) and bone colonization was monitored in the presence of estrogen for the indicated days and *in vivo* bioluminescent mouse images from representative animals at day 41 are shown. (**B**) Kaplan-Meier plot, (**C**) normalized photon flux plot (Error bars: s.e.m. (**D**) *In vitro* cell proliferation was quantified for MCF7 control and MCF7 GCP8 over-expressing cells.

Together the results demonstrate that experimental alteration of the GCP8 expression level has consequences for metastatic cell behavior in vivo.

Discussion

Discussion

In this study I have provided novel insight into the function of the γTuRC subunit GCP8. My work demonstrates that GCP8 regulates microtubule dynamics, most likely through its interaction with γTuRC, and also reveals a novel γTuRC-independent role of GCP8 in the regulation of the actomyosin network.

GCP8 and the γTuRC

To analyze the function of GCP8, the first aim was to determine how GCP8 binds to the γTuRC as no known functional region has been identified in GCP8. Therefore the identification of the γTuRC binding region and of other potential functional regions in GCP8 was crucial for achieving this aim.

In this work I have demonstrated that GCP8's γTuRC binding region comprises the N-terminal 1-111 amino acids. When a fragment consisting of this region was expressed in cells interaction with γTuRC by co-immunoprecipitation and co-localized with γ-tubulin at the centrosome was observed. Interestingly, this part of GCP8 also contained the most highly conserved region of the protein.

GCP8 and interphase microtubules

Since GCP8 was the only γTuRC subunit not required for mitotic spindle assembly, I investigated whether GCP8 might play a role in the regulation of the interphase microtubule network. Depletion of GCP8 through siRNA resulted in a strong increase in the rate of microtubule growth that was similar to previous work which

found that disruption of γTuRC also increased the microtubule growth rate (Bouissou et al., 2009). One explanation for this observation is that global inhibition of nucleation would cause an increase in the cellular concentration of free tubulin, which would, in turn, stimulate polymerization (Teixido-Travesa et al., 2012) (Sawin, 2004).

To address this I depleted the essential structural γTuRC subunits GCP2 or GCP6, however, this resulted in only a moderate increase in the rate of polymerization. Considering that GCP8 depletion does not disrupt γTuRC assembly/stability (Teixidó-Travesa et al., 2010) yet strongly stimulates microtubule growth it is reasonable to conclude that GCP8 might play a specific role in the regulation of microtubule plus end polymerization.

I also tested whether the increase in microtubule growth rate in the GCP8 depleted cells is γTuRC-dependent by co-depleting either GCP8/GCP2 or GCP8/GCP6. In both conditions the enhanced microtubule growth rate was reduced when compared to depletion of GCP8 alone. Therefore, the increase in microtubule polymerization in the GCP8 depleted cells is likely to be dependent on an intact γTuRC. In addition, full length GCP8 or GCP8 Nter over-expression had a similar stimulatory effect on the enhanced microtubule growth rate. This also supports the interpretation that GCP8 regulates microtubule plus ends through γTuRC.

Another avenue of investigation was the possibility that GCP8 regulates the microtubule plus end by stabilizing microtubules via direct binding to the microtubule lattice. Recent published work supports the concept that the γTuRC itself is a regulator for microtubule dynamics. A study in *Drosophila melanogaster* has shown that the γTuRC binds along the microtubule lattice where it limits the catastrophe and enhances the microtubule stability (Bouissou et al., 2009); however, to date in mammalian cells it has only been shown that the γTuRC binds to the astral microtubules during mitosis and has a antagonistic roles with EB1 in microtubule dynamics and spindle positioning (Bouissou et al., 2014). Therefore,

GCP8 could be localizing to the microtubule lattice with the γTuRC or the γTuRC through GCP8 and thereby influence the microtubule growth rate. Another possibility is that GCP8 with or without γTuRC directly binds to the microtubule plus end or regulates microtubule plus tip binding proteins. For example, *in vitro* experiments have shown that the amount of EB1 bound at the plus tip regulates the microtubule maturation and hence also the microtubule plus end dynamics (Maurer et al., 2014). Whatever the mechanism, it is most likely that the GCP8-dependent stimulation of microtubule growth rate is mediated by interaction with the γTuRC. This could be further tested by generating a GCP8 mutant with a specific defect in the region that binds to γTuRC.

Apart from binding to the microtubule lattice or plus end as discussed above, it is also possible that GCP8 regulates microtubule growth through γTuRC bound to the minus end. Two questions remain unanswered: first, how could GCP8 binding to γTuRC at the microtubule minus end regulate the behavior of the plus end? Second, why does both GCP8 depletion and over-expression stimulate the microtubule growth rate?

Regarding the first question, GCP8 binding to γTuRC could induce a conformational change in the γTuRC. Since γTuRC nucleates microtubules by providing a template, this conformational change could induce a subtle change in the structure of the microtubule and, as a consequence, favor the faster addition of new α- and β-tubulin at the plus end.

Regarding the second question, it is possible that the over-expression of GCP8 causes a dominant-negative effect by titration of an additional, unknown factor involved in γTuRC regulation, or that regulation of γTuRC by GCP8 requires a specific number of GCP8 molecules to interact with γTuRC.

In cells with reduced nucleation activity it is anticipated that the concentration of free tubulin would be elevated. Since I found that GCP-GCP8 over-expression

resulted in an inhibition of centrosomal microtubule nucleation, the increased microtubule polymerization rate under these conditions may also be an indirect effect of an increased concentration in free tubulin. Indeed, the increase in microtubule polymerization rate in cells overexpressing GCP8 was similar to cells with disrupted γTuRC, after depletion of GCP2 or GCP6.

Additional functions of GCP8

Since changes in microtubule plus end dynamics did not readily explain the adhesion defects and increased contractility observed in cells with altered GCP8 levels, I was interested in further investigating whether GCP8 might have a function beyond the regulation of γTuRC. Using different fixation methods I aimed to identify potentially novel subcellular localization of GCP8. With the exception of the well-documented GCP8 localization at the centrosome I also observed GCP8 staining in the nucleus. Both the staining for endogenous GCP8 as well as the over-expressed form of GFP-GCP8 were enriched in the nucleus during interphase, thus suggesting that this localization was specific. Unfortunately, no further investigations into the nuclear localization of GCP8 were conducted during my PhD project and the function of nuclear GCP8 remains currently unknown. Since a nuclear function may also be related to the depletion/over-expression phenotypes, one possible future avenue of research would be to specifically interfere with GCP8 nuclear localization and test whether this generates similar defects as observed by its depletion.

In cells that were pre-extracted before fixation I was able to observe localization of both the endogenous and GFP-tagged GCP8 along actin stress fibers. Furthermore, endogenous GCP8 was also detected at focal adhesion sites where actin stress fibers were anchored. In addition, GFP-GCP8 and the fragment GFP-GCP8 Cter, which does not interact with γTuRC, localized to the midbody. Since

only the Cterm fragment but not the Nterm fragment localized to the midbody, this might indicate that the C-terminus of GCP8 mediates this non-centrosomal localization.

In addition to U2OS cells I used BM20990 bone metastatic cells, a different cell model derived from the MCF7 breast cancer cell line. I chose to investigate the GCP8 localization in these cells as preliminary tests indicated that BM20990 cells express relatively high levels of GCP8 whereas other γTuRC subunit protein levels did not differ from U2OS cells. When I stained for GCP8 in BM20990 cells I observed the previously seen centrosomal and nuclear localization of GCP8, but also GCP8 localization at the cell cortex between cell-cell junctions. By contrast, GCP4 was detected only at the centrosome. Together, this suggests that GCP8 is localized to non-centrosomal sites via a mechanism that is independent of γTuRC. To test this more directly, I disrupted γTuRC by depletion of GCP2. Under these conditions the signals of GCP8 and GCP4 at the centrosome were abolished, whereas the GCP8 staining at the cell cortex between cell-cell junctions remained. Again, this suggests that GCP8 localization at this site is γTuRC independent. To further validate these novel non-centrosomal localizations of GCP8 and corroborate the specificity of the stainings, these experiments would have to be repeated with GCP8-depleted cells.

Together the localization experiments suggest that GCP8 might have a γTuRC-independent role at non-centrosomal sites.

GCP8 and the regulation of actomyosin

The most striking phenotype that I observed after GCP8 depletion or over-expression was a change in cell morphology. Cells appeared rounded and contractile with extensive plasma membrane blebbing. Based on over-expression

experiments, this appeared to be an effect that was predominantly mediated by the C-terminal part of GCP8, which does not bind to γTuRC.

Since these membrane blebs were not the result of apoptosis (previous work did not detect cell death after GCP8 RNAi; (Teixidó-Travesa et al., 2010)) and since I discovered that GCP8, but not γTuRC, localized to structures associated with actomyosin activity, GCP8 may play a role in the regulation of actomyosin, independent of its role in γTuRC regulation.

Indeed, cells were not able to adhere to the surface of the culture dish after either GCP8 depletion or over-expression, and also exhibited a spreading defect. The ability of cells grown as adherent cultures to attach and establish dynamic contacts with the substrate surface is important for their proliferation rate (Choi et al., 2015). This may explain why previous work noted a slight reduction in cell proliferation after GCP8 RNAi (Teixidó-Travesa et al., 2010).

Direct evidence for an increase in myosin-based contractility was obtained by two methods. First, GCP8 depletion caused an increase in MLC phosphorylation, a marker for myosin activity. Second, the cell rounding and blebbing defect could be rescued by treatment with the myosin inhibitor blebbistatin.

To test whether GCP8 may regulate myosin activity by physical interaction I performed pull-down assays. In *in vitro* assays with tagged GCP8 I observed a pull down of different myosins from cell lysates. Indeed the protein amount purified in the pull-down assay by GST-GCP8 was unexpectedly high. In the mass spec analysis I obtained a long list of proteins that included different myosins and other cytoskeletal proteins. For unknown reasons I was not able to detect any γTuRC subunits, however I was able to detect these by western blot analysis of the same samples.

In addition, Flag-tagged GCP8 was able to co-immunoprecipitate with GFP-MLC, which also supports the conclusion that GCP8 might play a role in MLC regulation.

Using either calyculina A or blebbistatin drug treatment that increased or decreased cell contractility, respectively, I was also able to show that the elevated microtubule growth rate after GCP8 depletion was independent of cell contractility. This could have been a factor if, for example, GCP8 would have a role in the previously described crosstalk between contractility and microtubule dynamics/stability (Joo and Yamada, 2014). For example, microtubule stabilization was shown to inhibit the positive RhoA regulator GEF-H1, thereby inhibiting contractility (Krendel et al., 2002).

Again, an unresolved question is why both GCP8 depletion and over-expression induced actomyosin-based contractility. The most likely explanation is that contractility depends on the correct GCP8 levels and that GCP8 over-expression could titrate out a binding partner that is important for the regulation of contractility, resulting in a similar phenotype as GCP8 depletion.

GCP8 and microtubule acetylation

Interestingly, the regulation of myosin contractility was correlated with changes in microtubule acetylation. Depletion of GCP8 gave rise to an increase in microtubule acetylation, indicating microtubule stabilization.

Recently, the regulation of microtubule acetylation has been linked to cell contractility via MYPT1 (myosin phosphatase target subunit 1), which was proposed to act as a molecular switch. When MYPT1 bound and dephosphorylated MLC or HDAC6, cellular contractility was decreased or HDAC6 activity was inhibited with enhanced acetylation of microtubules. Conversely, when MYPT1 was not bound to MLC, cellular contractility was enhanced due to increased phosphorylation of MLC, when not bound to MYPT1 and HDAC6 activity is increased, which promotes deacetylation of microtubules (Joo and Yamada, 2014).

Together, my data suggests that GCP8 affects these processes through MYPT1. For example, GCP8 might be needed for MYPT1 to dephosporylate MLC. Hence when GCP8 is depleted MYPT1 cannot dephosporylate MLC, which results in increased cellular contractility. Subsequently, excess of the MYPT1, which cannot act on MLC, might therefore have a stronger effect on inhibiting HDAC6, which then leads to an increase in microtubule acetylation.

Over-expression of GCP8 always resulted in a milder effect on cell contractility; hence the excess of GCP8 could have a dominant negative effect on the MYPT1 regulation of MLC phosphorylation and cause the milder increase in cellular contractility, while still enough MYPT1 is available to activate HDAC6 to prevent microtubule acetylation.

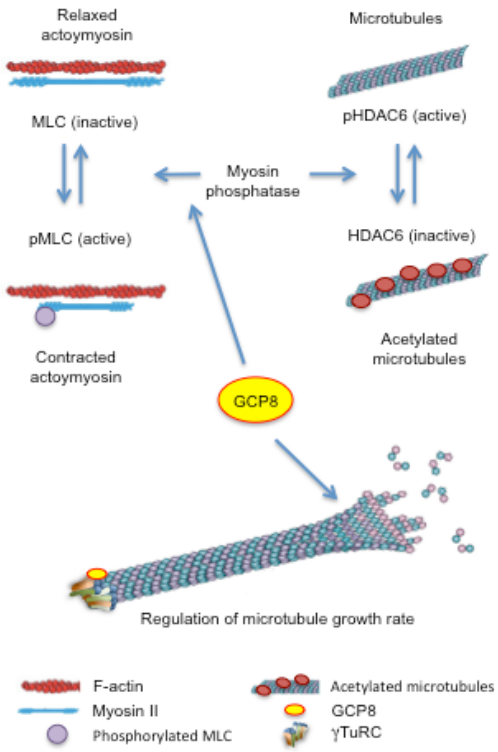

Figure 39. Proposed roles of GCP8.

Proposed roles of GCP8 in regulating contractility and microtubule acetylation, through interaction with the actomyosin network, as well as microtubule plus end growth, through interaction with γTuRC. MYPT1 is a regulator for MLC phosphorylation. GCP8 might promote the regulation of MLC by MYPT1, which limits cellular contractility. When this regulation is lost, for example by depletion of GCP8, then the excess of MYPT1 activity acts on HDAC6, which causes an increase in microtubule acetylation. Apart from the role of GCP8 in MYPT1 regulation, it also takes part in microtubule growth rate regulation. GCP8 acts through the γTuRC and increases microtubule growth rate. (Adapted from Joo and Yamada, 2014).

GCP8 and cell motility

Actomyosin regulation is important during cell migration. I therefore tested the influence of GCP8 on cell motility. Surprisingly, contrary to the results obtained in the 2D assay, GCP8 depleted or over-expressing cells moved faster into the matrix than the control cells in the 3D invasion assay. This could be due to the migration

mode used by cells with altered GCP8 levels. Directed migration on a 2D substrate surface requires cell polarization including dynamic assembly and disassembly of focal adhesions, whereas motility in a 3D environment can be achieved by either a polarized migration mode or by amoeboid motility. Amoeboid migration does not involve polarization and focal adhesions but depends on cortical contractility. Since changes in GCP8 expression level produce defects in cell adhesion and an increase in cell contractility, the cells may use the amoeboid migration mode to invade the collagen matrix.

GCP8 and Cancer

Since my results from the 2D and 3D migration assay suggested that the protein levels of GCP8 may be correlated with the migratory/invasive properties of cells, it can be speculated that GCP8 may have a role in metastasis. Interestingly and consistent with such a role, I found that GCP8 expression levels in different cancer cell lines were highly variable, whereas expression of other γTuRC subunits was consistent. Moreover, I demonstrated a role of GCP8 in cell motility *in vivo* using a mouse xenograft model. Why cells over-expressing GCP8 are less likely to colonize the bone could be explained in two ways: either the cells weren't able to adhere initially or, since they had an increased motility, they might have migrated away from the injection site and were therefore not able to colonize bone. This data provides an intriguing insight into the possibility that altering GCP8 levels can be used to modulate the metastatic potential of cancer cells.

In summary my data suggests that changing GCP8 protein levels in cells with an adhesion-dependent motility mode causes a switch to an amoeboid mode, which impacts metastatic cell behavior *in vitro* and *in vivo*.

Conclusions and Outlook

Based on the data acquired during my PhD I can hypothesize that GCP8 is an important dual-function regulator that on the one hand controls actomyosin contractility and microtubule acetylation and on the other hand controls microtubule plus end growth. Whereas regulation of the microtubule growth rate is most likely γTuRC dependent, actomyosin regulation seems to be γTuRC independent. Furthermore, by regulating both cell contractility and microtubule properties, GCP8 affects metastatic potential of cancer cells *in vivo*.

Insight into the mechanism by which GCP8 carries out these functions may allow modulation of this activity to inhibit metastasis.

For example, what is the molecular link between GCP8 and actomyosin regulation? Since my mass spec result did not yield conclusive evidence, further work identifying possible GCP8 interactors could answer how GCP8 regulates actomyosin. To identify such non-γTuRC binding partners, the BioID method could be an alternative approach (Roux et al., 2012). GCP8 or deletion mutants could be expressed in human cells as fusion proteins with BirA, which leads to the selective biotinylation of binding partners and other proteins that are in proximity to GCP8 in its native cellular environment. Biotinylated proteins would be affinity purified from lysates and candidates identified by mass spectrometry.

Apart from these molecular analyses, the role of GCP8 in metastasis needs to be studied in more detail. Further testing of the effects of both elevated and decreased levels of GCP8 in a larger panel of cancer cells and in different metastasis models needs to be performed in order to determine whether certain GCP8 expression levels are associated with a specific metastatic behavior.

Conclusions

- GCP8 is an important dual-function regulator that controls actomyosin contractility and microtubule acetylation on one hand, and microtubule plus end growth on the other hand

- Regulation of the microtubule growth rate most likely involves interaction with the γTuRC.

- Actomyosin regulation by GCP8 seems to be γTuRC independent

- Regulating both cell contractility and microtubule properties, GCP8 affects metastatic potential of cancer cells *in vitro* and *in vivo*.

References

Akhmanova, A., and Steinmetz, M.O. (2008). Tracking the ends: a dynamic protein network controls the fate of microtubule tips. Nat. Rev. Mol. Cell Biol. *9*, 309–322.

Akhmanova, A., and Steinmetz, M.O. (2010). Microtubule +TIPs at a glance. J. Cell Sci. *123*, 3415–3419.

Akhshi, T.K., Wernike, D., and Piekny, A. (2014). Microtubules and actin crosstalk in cell migration and division. Cytoskelet. Hoboken NJ *71*, 1–23.

Arnal, I., and Wade, R.H. (1995). How does taxol stabilize microtubules? Curr. Biol. CB *5*, 900–908.

Bahtz, R., Seidler, J., Arnold, M., Haselmann-Weiss, U., Antony, C., Lehmann, W.D., and Hoffmann, I. (2012). GCP6 is a substrate of Plk4 and required for centriole duplication. J. Cell Sci. *125*, 486–496.

Baquero, M.T., Hanna, J.A., Neumeister, V., Cheng, H., Molinaro, A.M., Harris, L.N., and Rimm, D.L. (2012). Stathmin expression and its relationship to microtubule-associated protein tau and outcome in breast cancer. Cancer *118*, 4660–4669.

Al-Bassam, J. (2002). MAP2 and tau bind longitudinally along the outer ridges of microtubule protofilaments. J. Cell Biol. *157*, 1187–1196.

Bettencourt-Dias, Mo., and Glover, D.M. (2007). Centrosome biogenesis and function: centrosomics brings new understanding. Nat. Rev. Mol. Cell Biol. *8*, 451–463.

Bos, J.L., Rehmann, H., and Wittinghofer, A. (2007). GEFs and GAPs: Critical Elements in the Control of Small G Proteins. Cell *129*, 865–877.

Bouissou, A., Vérollet, C., Sousa, A., Sampaio, P., Wright, M., Sunkel, C.E., Merdes, A., and Raynaud-Messina, B. (2009). γ-Tubulin ring complexes regulate microtubule plus end dynamics. J. Cell Biol. *187*, 327–334.

Bouissou, A., Vérollet, C., de Forges, H., Haren, L., Bellaïche, Y., Perez, F., Merdes, A., and Raynaud-Messina, B. (2014). γ-Tubulin Ring Complexes and EB1 play antagonistic roles in microtubule dynamics and spindle positioning. EMBO J. *33*, 114–128.

Bravo-Cordero, J.J., Hodgson, L., and Condeelis, J. (2012). Directed cell invasion and migration during metastasis. Curr. Opin. Cell Biol. *24*, 277–283.

Cassimeris, L.U., Wadsworth, P., and Salmon, E.D. (1986). Dynamics of microtubule depolymerization in monocytes. J. Cell Biol. *102*, 2023–2032.

Choi, W.J., Jung, J., Lee, S., Chung, Y.J., Yang, C.-S., Lee, Y.K., Lee, Y.-S., Park, J.K., Ko, H.W., and Lee, J.-O. (2015). Effects of substrate conductivity on cell morphogenesis and proliferation using tailored, atomic layer deposition-grown ZnO thin films. Sci. Rep. *5*.

Choi, Y.-K., Liu, P., Sze, S.K., Dai, C., and Qi, R.Z. (2010). CDK5RAP2 stimulates microtubule nucleation by the -tubulin ring complex. J. Cell Biol. *191*, 1089–1095.

Choudhary, C., Kumar, C., Gnad, F., Nielsen, M.L., Rehman, M., Walther, T.C., Olsen, J.V., and Mann, M. (2009). Lysine Acetylation Targets Protein Complexes and Co-Regulates Major Cellular Functions. Science *325*, 834–840.

Chrétien, D., Fuller, S.D., and Karsenti, E. (1995). Structure of growing microtubule ends: two-dimensional sheets close into tubes at variable rates. J. Cell Biol. *129*, 1311–1328.

Cronier, L., Crespin, S., Strale, P.-O., Defamie, N., and Mesnil, M. (2009). Gap junctions and cancer: new functions for an old story. Antioxid. Redox Signal. *11*, 323–338.

Etienne-Manneville, S., and Hall, A. (2002). Rho GTPases in cell biology. Nature *420*, 629–635.

Friedl, P. (2004). Prespecification and plasticity: shifting mechanisms of cell migration. Curr. Opin. Cell Biol. *16*, 14–23.

Gaggioli, C., and Sahai, E. (2007). Melanoma invasion ? current knowledge and future directions. Pigment Cell Res. *20*, 161–172.

González, M., Cambiazo, V., and Maccioni, R.B. (1998). The interaction of Mip-90 with microtubules and actin filaments in human fibroblasts. Exp. Cell Res. *239*, 243–253.

Goshima, G., Mayer, M., Zhang, N., Stuurman, N., and Vale, R.D. (2008). Augmin: a protein complex required for centrosome-independent microtubule generation within the spindle. J. Cell Biol. *181*, 421–429.

Guillet, V., Knibiehler, M., Gregory-Pauron, L., Remy, M.-H., Chemin, C., Raynaud-Messina, B., Bon, C., Kollman, J.M., Agard, D.A., Merdes, A., et al. (2011). Crystal structure of γ-tubulin complex protein GCP4 provides insight into microtubule nucleation. Nat. Struct. Mol. Biol. *18*, 915–919.

Gundersen, G.G. (2002). Microtubule capture: IQGAP and CLIP-170 expand the repertoire. Curr. Biol. CB *12*, R645–R647.

Hayashi, I., and Ikura, M. (2003). Crystal Structure of the Amino-terminal Microtubule-binding Domain of End-binding Protein 1 (EB1). J. Biol. Chem. *278*, 36430–36434.

Hernandez, F., García-García, E., and Avila, J. (2013). Microtubule depolymerization and tau phosphorylation. J. Alzheimers Dis. *37*, 507–513.

Hooper, S., Marshall, J.F., and Sahai, E. (2006). Tumor cell migration in three dimensions. Methods Enzymol. *406*, 625–643.

Hutchins, J.R.A., Toyoda, Y., Hegemann, B., Poser, I., Hériché, J.-K., Sykora, M.M., Augsburg, M., Hudecz, O., Buschhorn, B.A., Bulkescher, J., et al. (2010). Systematic analysis of human protein complexes identifies chromosome segregation proteins. Science *328*, 593–599.

Jacquemet, G., and Humphries, M.J. (2013). IQGAP1 is a key node within the small GTPase network. Small GTPases *4*, 199–207.

Janke, C., and Chloë Bulinski, J. (2011). Post-translational regulation of the microtubule cytoskeleton: mechanisms and functions. Nat. Rev. Mol. Cell Biol. *12*, 773–786.

Janski, N., Masoud, K., Batzenschlager, M., Herzog, E., Evrard, J.-L., Houlné, G., Bourge, M., Chabouté, M.-E., and Schmit, A.-C. (2012). The GCP3-interacting proteins GIP1 and GIP2 are required for γ-tubulin complex protein localization, spindle integrity, and chromosomal stability. Plant Cell *24*, 1171–1187.

Joo, E.E., and Yamada, K.M. (2014). MYPT1 regulates contractility and microtubule acetylation to modulate integrin adhesions and matrix assembly. Nat. Commun. *5*, 3510.

Kaverina, I., Krylyshkina, O., and Small, J.V. (1999). Microtubule targeting of substrate contacts promotes their relaxation and dissociation. J. Cell Biol. *146*, 1033–1044.

Keil, R., Wolf, A., Hüttelmaier, S., and Hatzfeld, M. (2007). Beyond regulation of cell adhesion: local control of RhoA at the cleavage furrow by the p0071 catenin. Cell Cycle Georget. Tex *6*, 122–127.

Kim, J., Nagami, S., Lee, K.-H., and Park, S.-J. (2014). Characterization of Microtubule-Binding and Dimerization Activity of Giardia lamblia End-Binding 1 Protein. PLoS ONE *9*, e97850.

Kitzing, T.M., Sahadevan, A.S., Brandt, D.T., Knieling, H., Hannemann, S., Fackler, O.T., Grosshans, J., and Grosse, R. (2007). Positive feedback between

Dia1, LARG, and RhoA regulates cell morphology and invasion. Genes Dev. *21*, 1478–1483.

Kollman, J.M., Zelter, A., Muller, E.G.D., Fox, B., Rice, L.M., Davis, T.N., and Agard, D.A. (2008). The structure of the gamma-tubulin small complex: implications of its architecture and flexibility for microtubule nucleation. Mol. Biol. Cell *19*, 207–215.

Kollman, J.M., Greenberg, C.H., Li, S., Moritz, M., Zelter, A., Fong, K.K., Fernandez, J.-J., Sali, A., Kilmartin, J., Davis, T.N., et al. (2015). Ring closure activates yeast γTuRC for species-specific microtubule nucleation. Nat. Struct. Mol. Biol. *22*, 132–137.

Krendel, M., Zenke, F.T., and Bokoch, G.M. (2002). Nucleotide exchange factor GEF-H1 mediates cross-talk between microtubules and the actin cytoskeleton. Nat. Cell Biol. *4*, 294–301.

Kumar, P., and Wittmann, T. (2012). +TIPs: SxIPping along microtubule ends. Trends Cell Biol. *22*, 418–428.

Leijnse, N., Oddershede, L.B., and Bendix, P.M. (2015). An updated look at actin dynamics in filopodia. Cytoskelet. Hoboken NJ *72*, 71–79.

Lüders, J. (2012). The amorphous pericentriolar cloud takes shape. Nat. Cell Biol. *14*, 1126–1128.

Lüders, J., and Stearns, T. (2007). Microtubule-organizing centres: a re-evaluation. Nat. Rev. Mol. Cell Biol. *8*, 161–167.

Lüders, J., Patel, U.K., and Stearns, T. (2006). GCP-WD is a γ-tubulin targeting factor required for centrosomal and chromatin-mediated microtubule nucleation. Nat. Cell Biol. *8*, 137–147.

Lyle, K., Kumar, P., and Wittmann, T. (2009). SnapShot: Microtubule regulators II. Cell *136*, 566, 566.e1.

Lynch, E.M., Groocock, L.M., Borek, W.E., and Sawin, K.E. (2014). Activation of the γ-Tubulin Complex by the Mto1/2 Complex. Curr. Biol. *24*, 896–903.

Maffini, S., Maia, A.R.R., Manning, A.L., Maliga, Z., Pereira, A.L., Junqueira, M., Shevchenko, A., Hyman, A., Yates Iii, J.R., Galjart, N., et al. (2009). Motor-Independent Targeting of CLASPs to Kinetochores by CENP-E Promotes Microtubule Turnover and Poleward Flux. Curr. Biol. *19*, 1566–1572.

Margolis, R.L. (1981). Role of GTP hydrolysis in microtubule treadmilling and assembly. Proc. Natl. Acad. Sci. U. S. A. *78*, 1586–1590.

Maurer, S.P., Cade, N.I., Bohner, G., Gustafsson, N., Boutant, E., and Surrey, T. (2014). EB1 Accelerates Two Conformational Transitions Important for Microtubule Maturation and Dynamics. Curr. Biol. *24*, 372–384.

Nakagawa, U., Suzuki, D., Ishikawa, M., Sato, H., Kamemura, K., and Imamura, A. (2013). Acetylation of α-tubulin on Lys40 is a widespread post-translational modification in angiosperms. Biosci. Biotechnol. Biochem. *77*, 1602–1605.

Nakamura, M., Yagi, N., Kato, T., Fujita, S., Kawashima, N., Ehrhardt, D.W., and Hashimoto, T. (2012). Arabidopsis GCP3-interacting protein 1/MOZART 1 is an integral component of the γ-tubulin-containing microtubule nucleating complex: Arabidopsis GIP1/MOZART1 in γTuRC. Plant J. *71*, 216–225.

Ng, D.H.J., Humphries, J.D., Byron, A., Millon-Frémillon, A., and Humphries, M.J. (2014). Microtubule-dependent modulation of adhesion complex composition. PloS One *9*, e115213.

Nguyen, D.X., Bos, P.D., and Massagué, J. (2009). Metastasis: from dissemination to organ-specific colonization. Nat. Rev. Cancer *9*, 274–284.

Olson, M.F., and Sahai, E. (2009). The actin cytoskeleton in cancer cell motility. Clin. Exp. Metastasis *26*, 273–287.

Pankov, R., Cukierman, E., Katz, B.Z., Matsumoto, K., Lin, D.C., Lin, S., Hahn, C., and Yamada, K.M. (2000). Integrin dynamics and matrix assembly: tensin-dependent translocation of alpha(5)beta(1) integrins promotes early fibronectin fibrillogenesis. J. Cell Biol. *148*, 1075–1090.

Ridley, A.J. (2001). Rho GTPases and cell migration. J. Cell Sci. *114*, 2713–2722.

Ridley, A.J., Schwartz, M.A., Burridge, K., Firtel, R.A., Ginsberg, M.H., Borisy, G., Parsons, J.T., and Horwitz, A.R. (2003). Cell migration: integrating signals from front to back. Science *302*, 1704–1709.

Roux, K.J., Kim, D.I., Raida, M., and Burke, B. (2012). A promiscuous biotin ligase fusion protein identifies proximal and interacting proteins in mammalian cells. J. Cell Biol. *196*, 801–810.

Sahai, E. (2005). Mechanisms of cancer cell invasion. Curr. Opin. Genet. Dev. *15*, 87–96.

Sawin, K.E. (2004). Microtubule dynamics: faint speckle, hidden dragon. Curr. Biol. CB *14*, R702–R704.

Schölz, C., Weinert, B.T., Wagner, S.A., Beli, P., Miyake, Y., Qi, J., Jensen, L.J., Streicher, W., McCarthy, A.R., Westwood, N.J., et al. (2015). Acetylation site

specificities of lysine deacetylase inhibitors in human cells. Nat. Biotechnol. *33*, 415–423.

Skoge, R.H., Dölle, C., and Ziegler, M. (2014). Regulation of SIRT2-dependent α-tubulin deacetylation by cellular NAD levels. DNA Repair *23*, 33–38.

Teixidó-Travesa, N., Villén, J., Lacasa, C., Bertran, M.T., Archinti, M., Gygi, S.P., Caelles, C., Roig, J., and Lüders, J. (2010). The gammaTuRC revisited: a comparative analysis of interphase and mitotic human gammaTuRC redefines the set of core components and identifies the novel subunit GCP8. Mol. Biol. Cell *21*, 3963–3972.

Teixido-Travesa, N., Roig, J., and Luders, J. (2012). The where, when and how of microtubule nucleation - one ring to rule them all. J. Cell Sci. *125*, 4445–4456.

Tilney, L.G., Bryan, J., Bush, D.J., Fujiwara, K., Mooseker, M.S., Murphy, D.B., and Snyder, D.H. (1973). Microtubules: evidence for 13 protofilaments. J. Cell Biol. *59*, 267–275.

Verollet, C. (2006). Drosophila melanogaster -TuRC is dispensable for targeting -tubulin to the centrosome and microtubule nucleation. J. Cell Biol. *172*, 517–528.

Wang, H., Tan, Q., Yang, B.Y., Zou, X., and Yang, L. (2011). [Research progress of tumor cell migration strategy and the migration transition mechanism]. Sheng Wu Yi Xue Gong Cheng Xue Za Zhi J. Biomed. Eng. Shengwu Yixue Gongchengxue Zazhi *28*, 1251–1256.

Wang, Z., Wu, T., Shi, L., Zhang, L., Zheng, W., Qu, J.Y., Niu, R., and Qi, R.Z. (2010). Conserved motif of CDK5RAP2 mediates its localization to centrosomes and the Golgi complex. J. Biol. Chem. *285*, 22658–22665.

Wiese, C., and Zheng, Y. (2000). A new function for the gamma-tubulin ring complex as a microtubule minus-end cap. Nat. Cell Biol. *2*, 358–364.

Wiese, C., and Zheng, Y. (2006). Microtubule nucleation: -tubulin and beyond. J. Cell Sci. *119*, 4143–4153.

Wittmann, T. (2003). Regulation of leading edge microtubule and actin dynamics downstream of Rac1. J. Cell Biol. *161*, 845–851.

Xiong, Y., and Oakley, B.R. (2009). In vivo analysis of the functions of -tubulin-complex proteins. J. Cell Sci. *122*, 4218–4227.

Yano, H. (2006). [Signal crosstalk between cell-substratum adhesion and cell-cell adhesion]. Tanpakushitsu Kakusan Koso. *51*, 660–665.